The transcription factor TRF2 has a unique function in regulating cell cycle and apoptosis

Adi Kedmi[*], Anna Sloutskin[*], Natalie Epstein[*], Lital Gasri-Plotnitsky[*], Debby Ickowicz[*], Irit Shoval[*], Tirza Doniger[*], Eliezer Darmon[*], Diana Ideses[*], Ziv Porat[†], Orly Yaron[*], and Tamar Juven-Gershon[*1]

[*] The Mina and Everard Goodman Faculty of Life Sciences, Bar-Ilan University, Ramat Gan 5290002, Israel; and

[†] The Flow Cytometry Unit, Life Sciences Core Facilities, Weizmann Institute of Science, Rehovot 7610001, Israel

[1] Correspondence: The Mina and Everard Goodman Faculty of Life Sciences, Bar-Ilan University, Ramat Gan 5290002, Israel. E-mail: tamar.gershon@biu.ac.il

ABSTRACT

Background: Diverse biological processes and transcriptional programs are regulated by RNA polymerase II (Pol II), which is recruited by the general transcription machinery to the core promoter to initiate transcription. TRF2 (TATA-box-binding protein-related factor 2) is an evolutionarily conserved general transcription factor that is essential for embryonic development of *Drosophila melanogaster*, *C. elegans*, zebrafish and *Xenopus*. Nevertheless, the cellular processes that are regulated by TRF2 are largely underexplored.

Results: Here, using *Drosophila* Schneider cells as a model, we discovered that TRF2 regulates apoptosis and cell cycle progression. We show that TRF2 knockdown results in increased expression of distinct pro-apoptotic genes and induces apoptosis. Using flow cytometry, high-throughput microscopy and advanced imaging-flow cytometry, we demonstrate that TRF2 regulates cell cycle progression and exerts distinct effects on G1 and specific mitotic phases. RNA-seq analysis revealed that TRF2 controls the expression of *Cyclin E* and the mitotic cyclins, *Cyclin A*, *Cyclin B* and *Cyclin B3*, but not *Cyclin D* or *Cyclin C*. To identify proteins that could account for the observed regulation of these cyclin genes, we searched for TRF2-interacting proteins. Interestingly, mass spectrometry analysis of TRF2-containing complexes identified GFZF, a nuclear glutathione S-transferase implicated in cell cycle regulation, and Motif 1 binding protein (M1BP). TRF2 has previously been shown to interact with M1BP and M1BP has been shown to interact with GFZF. Furthermore, available ChIP-exo data revealed that TRF2, GFZF and M1BP co-occupy the promoters of TRF2-regulated genes. Using RNAi to knockdown the expression of either M1BP, GFZF, TRF2 or their combinations, we demonstrate that although GFZF and M1BP interact

with TRF2, it is TRF2, rather than GFZF or M1BP, that is the main factor regulating the expression of *Cyclin E* and the mitotic cyclins.

Conclusions: Our findings uncover a critical and unanticipated role of a general transcription factor as a key regulator of cell cycle and apoptosis.

Keywords

Basal transcription machinery, RNA polymerase II, gene expression, TATA box-binding protein (TBP), TBP-related factor 2 (TRF2), cyclin genes.

BACKGROUND

Multiple biological processes and transcriptional programs are regulated by RNA polymerase II (Pol II). The initiation of transcription of protein-coding genes and distinct non-coding RNAs occurs following the recruitment of Pol II to the core promoter region by the general/basal transcription machinery (1-4). The core promoter, which directs accurate initiation of transcription and encompasses the transcription start site (TSS), may contain short DNA sequence elements/motifs, which confer specific properties to the core promoter (1, 4-10). The first step in the recruitment of Pol II to initiate transcription is the binding of TFIID, which is composed of TATA-box-binding protein (TBP) and TBP-associated factors. Remarkably, although TBP is considered a universal general transcription factor, robust Pol II transcription is observed in mouse TBP-/- blastocysts, indicating the existence of TBP-independent Pol II transcription *in vivo* (11). The complexity of transcription is also manifested by the existence of diverse transcriptional regulators,

73 among which are the TBP family members. There are three TBP family members in
74 *Drosophila melanogaster*: TBP, TRF1 and TRF2 (reviewed in (12-16)). TRF1, the
75 first *Drosophila* TBP family member identified, is insect specific (17). An evolutionary
76 conservation analysis indicated that TRF2 (also known as TLP (TATA-like protein),
77 TLF (TBP-like factor), TRP (TBP-related protein) and TBPL1 (TBP-like 1)), is highly
78 conserved in evolution (12, 18-22) and is present in all bilaterian organisms, but not
79 in any of the non-bilaterian genomes available (19). It was further discovered that
80 TRF2, which is involved in Pol II transcription, evolved by duplication of the TBP
81 gene (19). Yet, unlike TBP and TRF1, TRF2 does not bind TATA-box containing
82 promoters (19, 20, 22). There are two *Drosophila* TRF2 protein isoforms that result
83 from an internal translation initiation: the evolutionarily conserved short isoform (632
84 aa; typically referred to as "TRF2") and a long *Drosophila*-only isoform (1715 aa), in
85 which the same short amino acid sequence is preceded by an N-terminal domain
86 (23). TRF2 affects early embryonic development of *Drosophila*, *C. elegans*, zebrafish
87 and *Xenopus*, differentiation and morphogenesis (23-32). Mouse TRF2 is essential
88 for spermiogenesis (33-35).

89 One of the open questions in the transcriptional regulation field is what are the
90 cellular functions of TRF2. Despite its importance in development, the cellular
91 processes that are regulated by TRF2 remain largely underexplored. To identify and
92 characterize the cellular processes that are regulated by TRF2, we used *Drosophila*
93 S2R+ cells as a model and knocked-down the expression of TRF2. We discovered
94 that reduced expression of TRF2 (but not TBP or TRF1) results in apoptosis and
95 increased expression of key, yet not all, pro-apoptotic genes (including *rpr, hid, p53*),
96 suggesting this is not a general stress response. Surprisingly, not only that TRF2
97 regulates apoptotic cell death, reduced expression of TRF2 (but not its family

98 members, TBP or TRF1), exerts distinct effects on G1, G2/M and specific mitotic
99 phases, as demonstrated by quantitative high-throughput imaging flow cytometry.
100 We further discovered that TRF2 controls the expression of *Cyc E* and the mitotic
101 *Cyc A*, *Cyc B* and *Cyc B3* genes. Using mass spectrometry analyses of TRF2-
102 interacting proteins and available ChIP-exo data, we demonstrate the co-occupancy
103 of TRF2, GFZF (GST-containing FLYWCH zinc-finger protein) and M1BP (motif 1
104 binding protein) in the majority of promoters bound by each of the three factors.
105 Remarkably, the promoters of the TRF2-regulated mitotic cyclins and *Cyclin E* are
106 bound by the three factors, whereas the promoters of *Cyclin C* and *Cyclin D*, which
107 are not regulated by TRF2, are not bound. Furthermore, the Motif 1 sequence
108 element is enriched in the promoters of genes bound by all three proteins,
109 suggesting the involvement of GFZF and M1BP as co-factors in TRF2-regulated cell
110 cycle progression. Moreover, we demonstrate that TRF2, rather than M1BP or
111 GFZF, is the main factor that regulates the expression of the mitotic cyclins and
112 *Cyclin E*. Importantly, while general/basal transcription factors might be viewed as
113 having a somewhat “generic” role, our findings emphasize the unique, unanticipated
114 functions of *Drosophila* TRF2 as an essential factor for cell cycle progression and
115 apoptotic cell death.

116 RESULTS

117 Knockdown of TRF2 expression results in apoptotic cell death and induced
118 expression of key pro-apoptotic genes

119 The TBP-related transcription factor TRF2 is a key general/basal transcription factor
120 (reviewed in (12-16)), yet the cellular processes that are regulated by TRF2 remain
121 largely underexplored. To investigate the cellular functions of TRF2, we used

122 *Drosophila* S2R+ cells as a model, and knocked down its expression by RNAi using
123 non-overlapping dsRNA probes (Additional file 1: Figure S1a). TBP knockdown was
124 used as a control throughout this study. The resulting reduction in protein expression
125 was verified by western blot analysis (Additional file 1: Figure S1b, c). We
126 consistently observed significant cell death following TRF2 knockdown, as evident by
127 microscopic examination and by the reduced amounts of total RNA purified from
128 TRF2-RNAi treated cells, as compared to mock-treated cells. To specifically
129 investigate whether TRF2 plays an important role in apoptosis, we performed
130 Annexin V/PI analysis to detect early and late apoptotic cell death by flow cytometry
131 analysis. PI is excluded from cells with intact membranes, while dead and damaged
132 cells have membranes that are permeable to PI. Annexin V binds phospholipids that
133 are exposed in cells undergoing apoptosis. Hence, cells that are both Annexin V and
134 PI negative are considered viable, while cells that are in early apoptosis are Annexin
135 V positive and PI negative, and cells that are in late apoptosis or already dead are
136 both Annexin V and PI positive. S2R+ cells were incubated for three days with either
137 one of the four non-overlapping dsRNA probes directed against *Trf2*, a dsRNA probe
138 against *Tbp*, a dsRNA probe against *Trf1* or a dsRNA probe against the
139 homeodomain transcription factor *exd*, as a negative control. Cells were harvested
140 and stained with Annexin-V FITC/PI. Approximately 30% of cells stain positive for
141 Annexin V following TRF2 knockdown by the four different dsRNA probes, ~2 fold
142 higher than the mock and the exd-RNAi treated cells (Fig. 1). Notably, cell death
143 induced by TBP or TRF1 dsRNA probes (an average of 20%) was not as
144 pronounced as the cell death induced by either of the four TRF2 dsRNA probes.
145 These findings emphasize the unique effects of TRF2, as compared to TBP, on
146 apoptosis.

147 To identify the targets that are unique to TRF2, we used RNAi to knockdown
148 either TRF2 or TBP in *Drosophila* S2R+ cells and performed RNA-seq analysis at
149 two time points, 48h and 72h. In order to further understand how TRF2 knockdown
150 results in cell death, we searched our RNA-seq data for pro-apoptotic genes that are
151 regulated by TRF2. The inhibitor of apoptosis protein (IAP) family has already been
152 shown to play an important role in cell survival (reviewed in (36-38)). *Drosophila*
153 Death-associated IAP-1 (DIAP1), a key member of the IAP family, inhibits apoptosis
154 by binding to the active Caspase 9-like Dronc, and functioning as an E3-ubiquitin
155 ligase to promote its degradation. The *reaper* (*rpr*), *head involution defective* (*hid*),
156 and *grim* genes encode IAP antagonists that bind DIAP1, disrupt its interactions with
157 caspases and target it for degradation, resulting in caspase activation and cell death.
158 Scylla (*scyl*) has been implicated in developmental cell death (39). Indeed, the RNA-
159 seq analysis revealed a significant upregulation of *rpr* and *scyl* (Additional file 2:
160 Table S1). We thus decided to knockdown either TRF2 (probes #1 and #2), exd,
161 TBP or TRF1 and examine by reverse transcription-qPCR the expression of multiple
162 genes implicated in the apoptotic machinery: the IAP antagonists *rpr*, *hid* and *grim*
163 (reviewed in (37)), *scyl* (39), the BCL-2 family members *buffy* (40) and *Death*
164 *executioner Bcl-2* (*Debcl*) (41-44), and the Caspase 9-like *Dronc* (reviewed in (37)).
165 Remarkably, reducing the expression levels of TRF2 (but not exd, TBP or TRF1)
166 resulted in increased expression levels of *rpr*, *hid* and *scyl* (Fig. 2a). The detected
167 increase in *Buffy* expression levels was not statistically significant. The expression of
168 *grim*, *Debcl* and *Dronc* was not significantly altered by TRF2 knockdown (Fig. 2a),
169 suggesting that this is not a general stress response, and that TRF2 specifically
170 regulates the expression of distinct, but not all, pro-apoptotic genes.

171 The p53 tumor suppressor gene is a key regulator of both cell cycle
172 progression and programmed cell death (reviewed, for example, in (45, 46)). p53 is
173 expressed at low levels in S2R+ cells (www.flybase.org). Surprisingly, the RNA-seq
174 analysis revealed its upregulation upon TRF2 knockdown (Additional file 2: Table
175 S1). Examination of p53 expression by reverse transcription-qPCR following
176 knockdown of either TRF2 (probes #1 and #2) or TBP reproduced the upregulation
177 trend of p53 expression by TRF2. Notably, TBP knockdown did not alter the
178 expression of p53, manifesting the unique characteristics of gene regulation via
179 TRF2. Interestingly, it was previously demonstrated that p53 regulates the
180 expression of *rpr* and *hid*, which in turn, induce apoptosis (47, 48). Hence, it is
181 possible that the observed upregulation of *rpr* and *hid* following the knockdown of
182 TRF2 (Fig. 2a, b) is mediated via p53. Unfortunately, multiple attempts to reduce the
183 levels of endogenous p53 by two different dsRNA probes, were unsuccessful. Thus,
184 one cannot exclude the possibility that the increased expression of p53 following
185 TRF2 knockdown, may partially contribute to the upregulation of *rpr* and *hid*
186 expression.
187
188 **TRF2 exerts distinct effects that are independent of TBP**
189 TRF2 may repress transcription involving TBP or TFIID, probably by recruiting TFIIA
190 (20, 49). One can suggest that TRF2 is, in some respects, antagonistic to TBP, and
191 the observed upregulation of pro-apoptotic genes following TRF2 knockdown (Fig. 2)
192 results from TBP activity, which is no longer obstructed by TRF2. To examine
193 whether the observed upregulation of *rpr* and *hid* results from TBP activity, we
194 overexpressed TBP in S2R+ cells that were either incubated with TRF2 dsRNA
195 probes or mock treated. Although overexpression of TBP was clearly evident (>100

196 fold; Additional file 3: Figure S2), no differences in the levels of *rpr* and *hid* were
197 observed upon its overexpression (Additional file 3: Figure S2). Furthermore,
198 overexpression of TBP following TRF2 knockdown did not alter *rpr* or *hid* expression.
199 Thus, we conclude that the observed upregulation of *rpr* and *hid* following TRF2
200 knockdown results from the activity of TRF2 as a unique transcription factor, rather
201 than a TBP antagonist.
202
203 **Knockdown of endogenous TRF2 expression results in altered cell cycle**
204 **distribution and G1 arrest**
205 To identify specific cellular processes that are regulated by TRF2, we performed
206 Gene Ontology (GO) terms analysis of genes that were either downregulated or
207 upregulated following TRF2 knockdown (using string.db.org). Surprisingly, we
208 discovered that genes that were downregulated following TRF2 knockdown are
209 enriched for cell cycle and mitotic cell cycle processes, while genes that were
210 upregulated following TRF2 knockdown are enriched for response to stimulus and
211 stress (Additional file 2: Table S1). Interestingly, while the number of genes that were
212 downregulated was only half of the number of the upregulated genes following TRF2
213 knockdown (337 vs. 684 genes, respectively), the enrichment scores ($-\log_{10}$(P
214 values)) of the downregulated genes were 5-fold higher. We thus decided to
215 examine the effects of TRF2 knockdown on cell cycle distribution. To knockdown the
216 expression of the endogenous genes, S2R+ cells were incubated for three days with
217 dsRNA probes against *Trf2*, *Tbp*, *Trf1* or *exd*, as a negative control. Cells were
218 harvested, fixed and analyzed by flow cytometry. Control S2R+ cells display a
219 normal profile with an average of ~31% of cells in G1 phase and with an average of
220 ~34% of cells in G2/M phase, similarly to mock treated cells (which were processed

221 similarly, but were not incubated with any dsRNA; Fig. 3). Following TRF2
222 knockdown by either one of the four dsRNA probes, we observed a distinct decrease
223 in the fraction of cells in G2/M phase (an average of ~20%), as well as the fraction of
224 cells in S phase (an average of ~20%) with a concomitant increase in the fraction of
225 cells in G1 phase (an average of ~55%). Remarkably, these effects are unique to
226 TRF2 knockdown, as the knockdown of its family members TBP or TRF1 resembles
227 the cell cycle distribution of control and mock treated cells (Fig. 3).
228 Our RNA-seq analysis reveals subsets of genes that are involved in S and
229 G2/M phases. In addition, the cell cycle analysis indicates that TRF2 plays a role in
230 S and/or G2/M phases. To determine if TRF2 affects cell cycle progression to S
231 phase, S2R+ cells were arrested in G1 with 1mM hydroxyurea (HU) for 18h following
232 knockdown of either TRF2 (dsRNA probes #1 and #2) or TBP, and then released to
233 cycle by replacing the medium with fresh medium. As can be seen in Figure 4, HU
234 treatment (0h) resulted in accumulation of cells in G1 (~55%). Two hours following
235 the release, mock treated cells returned to cycle (indicated by the decrease in the
236 number of cells in G1), and the fraction of cells in S and G2/M increased. Similarly,
237 cells in which TBP was depleted by RNAi, returned to cycle. Surprisingly, unlike
238 mock or TBP RNAi-treated cells, cells in which TRF2 was depleted by either one of
239 the two probes, remained in G1 (~55%) and did not return to cycle (Fig. 4, Additional
240 file 4: Figure S3). Moreover, even 8h following the removal of HU, cells in which
241 TRF2 was knocked-down remained G1-arrested. Our findings imply that
242 endogenous TRF2 is involved in progression into S phase.
243
244
245

246 **TRF2 regulates the expression of specific cyclin genes**

247 To further explore the connection between TRF2 and cell cycle progression, we
248 turned to our RNA-seq data for cell cycle-related genes that may be influenced by
249 knockdown of TRF2. We discovered that following TRF2 knockdown, the expression
250 of the *Cyc A*, *Cyc B*, *Cyc B3* and *Cyc E* cell cycle regulators was significantly
251 reduced (over 2.3-fold). Notably, the expression levels of *Cyc C* and *Cyc D* were
252 unchanged (Additional file 2: Table S1). In order to verify the effect of TRF2
253 knockdown on the expression of these genes, reverse transcription-qPCR analysis
254 of endogenous cyclin genes was performed on mock, TRF2 (probes #1 and #2), exd,
255 TBP or TRF1 RNAi-treated cells. Knockdown of TRF2 by either probe #1 or #2
256 significantly reduces the expression of *Cyc A*, *Cyc B* and Cyc *B3*, as compared to
257 mock treated cells, much more than knockdown of TBP or TRF1 (Fig. 5a). As there
258 was a difference between the effects of probe #1 and #2 on *Cyc E* expression, 4
259 non-overlapping TRF2 dsRNA probes were used to assess the effect of TRF2
260 knockdown on *Cyc E* expression (Fig. 5b). Notably, each of the 4 non-overlapping
261 TRF2 dsRNA probes reduces *Cyc E* expression. Unlike *Cyc D* (which is required for
262 G1 progression (50, 51)), the expression of *Cyc E* (which promotes G1-S transition
263 (52, 53)) was reduced following TRF2 knockdown (Fig. 5a, b). We next tested
264 whether TRF2 knockdown affects the protein levels of Cyc A, Cyc B and Cyc E.
265 Unfortunately, we were unable to detect endogenous Cyc A and Cyc B protein
266 expression using publicly available anti- *Drosophila* Cyc A and Cyc B antibodies
267 (data not shown). Remarkably, using anti-*Drosophila* Cyc E antibodies, we observed
268 a distinct reduction in Cyc E protein levels following knockdown of TRF2 (but not
269 TBP), using both TRF2 probes (Fig. 5c), further suggesting that TRF2 regulates G1-
270 S transition by modulating the expression of *Cyc E*.

271 **TRF2 regulates distinct mitotic phases**

272 We were intrigued by the downregulation of the mitotic cyclin gene expression (*Cyc*
273 *A*, *Cyc B* and *Cyc B3*) following TRF2 knockdown (Fig. 5a) and decided to explore
274 the effect of TRF2 downregulation on mitotic phases. To this end, we knocked-down
275 the expression of TRF2 or TBP and stained cells for mitotic chromatin (anti-phospho-
276 Histone H3 (Ser10)), DNA (Hoechst) and filamentous Actin (Phalloidin). These
277 allowed us to analyze the fraction of cells in mitosis following TRF2 knockdown (Fig.
278 6a). To determine the number of mitotic cells, we developed a pipeline to
279 automatically detect the Hoechst and phospho-Histone H3 signals. Notably, there
280 was a reduction in the number of cells undergoing mitosis following TRF2
281 knockdown, as compared to mock or TBP RNAi treated cells (Fig. 6b).

282 To explore the effect of TRF2 on G2/M, we sought to synchronize cells in
283 G2/M. Unfortunately, we were unable to synchronize cells in G2/M in a reversible
284 manner (see methods), and thus we could not perform G2/M block-release
285 experiments. Nevertheless, we succeeded in discerning the effects of TRF2 on
286 specific mitotic phases by employing advanced imaging-flow cytometry analysis
287 (ImageStreamX mark II imaging flow-cytometer, Amnis Corp, Seattle, WA, Part of
288 EMD Millipore). Imaging-flow cytometry analysis combines the high-quality imaging
289 and functional insights of microscopy with the speed, sensitivity, and phenotyping
290 abilities of flow cytometry. We knocked down the expression of TRF2 or TBP and
291 stained cells with anti-phospho-Histone H3 (Ser10) antibodies and Hoechst. A total
292 of 40,000 cells of each treatment were analyzed by an ImageStream flow cytometer
293 to determine the number of cells in each mitotic phase, according to their nuclear
294 morphology (Fig. 6c-f, Additional file 5: Figure S4, Additional file 6: Table S2).
295 Remarkably, although 40,000 cells were analyzed in each experiment, only a few

296 hundred cells were mitotic, and following TRF2 knockdown there was an even bigger
297 reduction in the total number of mitotic cells (Fig. 6b, d). Notably, despite the overall
298 reduction in the mitotic cell population, knockdown of TRF2 (but not TBP) resulted in
299 a significant accumulation of cells in anaphase and telophase (Fig. 6e, f).
300 To validate the accurate identification of mitotic cells, we used Colchicine as a
301 control. Colchicine treatment resulted in accumulation of cells in mitosis, specifically
302 in anaphase (Fig. 6e). Multiple studies have shown that Colchicine disrupts the
303 metaphase to anaphase transition (see for example, (54)), yet, the increase in
304 anaphase has also been documented (55). Furthermore, it is established that
305 different cell types behave differently during mitosis in the presence of drugs that
306 disrupt microtubules function (56). Interestingly, morphological examination of the
307 Colchicine-treated S2R+ cells indicated aberrant DNA staining patterns and mal-
308 oriented clumped chromosomes in prophase, metaphase and anaphase cells
309 (Additional file 7: Figure S5), in line with the absence of a spindle. Notably, mal-
310 oriented un-centered chromosomes, such as those observed in Colchicine-treated
311 cells, were not observed in TRF2-RNAi treated cells.
312
313 **The effects of TRF2 knockdown on cyclin gene expression correlates with the**
314 **promoter occupancies of TRF2 and its co-factors GFZF and M1BP**
315 To better understand how TRF2 regulates the expression of the cyclin genes, we
316 turned our attention to TRF2-interacting proteins. TRF2 was recently shown to
317 interact with M1BP (motif 1 binding protein) (57). Interestingly, M1BP was recently
318 demonstrated to interact with GFZF, a nuclear glutathione S-transferase protein that
319 has been implicated in cell cycle regulation (58). We suspected that GFZF may
320 interact with TRF2. Indeed, using FLAG immuno-affinity purification from FLAG-HA

321 TRF2-inducible S2R+ cells followed by mass spectrometry analysis, we discovered
322 that both M1BP and GFZF are in complex with the evolutionarily conserved TRF2
323 (also known as short TRF2), but not with the long *Drosophila*-only TRF2 isoform or
324 with TBP (Table 3 and Additional file 8: Table S3). This prompted us to examine the
325 occupancy of TRF2, M1BP and GFZF in the vicinity of the TSSs (-100 to +100
326 relative to the TSS) of TRF2-regulated cyclin genes, using publicly available TRF2,
327 M1BP and GFZF ChIP-exo analyses in *Drosophila* S2R+ cells (GSE97841,
328 GSE105009) (57, 58). We examined the number of bound sites, the average peak
329 scores and the maximum peak scores of cyclin genes and several ribosomal protein
330 genes for comparison (Table 4). As expected, M1BP, TRF2 and GFZF co-occupy
331 the promoters of the ribosomal protein genes. Interestingly, while M1BP occupies the
332 -100 to +100 regions of all the examined cyclin genes, both TRF2 and GFZF occupy
333 the -100 to +100 regions of *Cyc A*, *Cyc B*, *Cyc B3* and *Cyc E*, and to a lesser extent
334 the promoters of *Cyc C* and *Cyc D*, which are not regulated by TRF2. The
335 occupancies of the three proteins is especially striking in the vicinities of the *Cyc B*
336 and *Cyc B3* TSSs. Thus, the effects of TRF2 knockdown on cyclin gene expression
337 generally correlate with the occupancies of both TRF2 and GFZF in the -100 to +100
338 regions of *Cyc A*, *Cyc B*, *Cyc B3* and *Cyc E.*
339
340 To characterize the co-occupancies of TRF2, GFZF and M1BP in a genome-
341 wide manner, we examined the binding of each factor to *Drosophila* promoter
342 regions (± 50 bp relative to FlyBase annotated TSSs). Remarkably, a major fraction
343 of promoters is bound by all three transcription factors (Fig. 7a). Reassuringly, the
344 co-bound promoters include the TRF2-regulated *Cyc A*, *Cyc B*, *Cyc B3* and *Cyc E*,
345 but not *Cyc C* and *Cyc D* promoters, which are not regulated by TRF2.

346 To better decipher the characteristics of the co-bound promoters, we used MEME
347 (59) to detect enriched sequence motifs. Interestingly, the top enriched motif in
348 promoters that are bound by all three proteins (Fig. 7b) closely resembles Ohler
349 Motif 1 (60), also detected in M1BP ChIP-exo analysis (57). We next analyzed the
350 core promoter composition of the co-bound promoters, using the ElemeNT algorithm
351 (61). Strikingly, the co-bound promoters are depleted for the TATA-box motif and
352 enriched for the TCT and Motif 1 core promoter elements, as compared to the
353 genomic distribution of core promoter elements (Fig. 7c).
354 To examine the contribution of M1BP and GFZF to the effect of TRF2
355 knockdown on cyclin gene expression, we used RNAi to knockdown the expression
356 of either M1BP, GFZF, TRF2 or their combinations. The use of each of the dsRNA
357 probes resulted in a significantly reduced expression of the targeted gene (Fig. 7d).
358 Surprisingly, M1BP knockdown resulted in increased expression of *Trf2*, *gfzf* and
359 *Cyc E*. Since both TRF2 and M1BP were previously shown to affect the expression
360 of ribosomal protein genes (32, 62), we tested whether their knockdown affects the
361 expression of several ribosomal target genes, namely, *RpL30*, *RpLP1* and *RpLP2*.
362 While TRF2 and GFZF knockdown did not affect their expression, M1BP knockdown
363 resulted in significantly increased expression of *RpLP2* (Additional file 9: Figure
364 S6a). Notably, this effect was not general, but rather specific to distinct cyclin and
365 ribosomal protein genes (Fig. 7d, e and Additional file 9: Figure S6), as the
366 expression of *CG12493* and *Sgll*, two previously identified M1BP targets (62), was
367 reduced following M1BP knockdown (Additional file 9: Figure S6b).
368 The expression levels of *Cyc A* and *Cyc B* were specifically reduced following TRF2
369 knockdown, but not following GFZF or M1BP knockdown (Fig. 5a and Fig. 7d, e).
370 *Cyc D* expression was not affected by either of these single factor knockdowns (Fig.

371 7d), as in Figure 5. As can be observed by TRF2 knockdown, as well as the
372 combined knockdown of TRF2, GFZF and M1BP, the expression pattern of *Cyc A*
373 and *Cyc B* are mostly influenced by TRF2 knockdown. *Cyc E* exhibits a composite
374 pattern: it is reduced following TRF2 knockdown, but the combined knockdowns of
375 TRF2 and M1BP or GFZF seem to restore its expression as compared to mock
376 treatment. Notably, *Cyc D* expression pattern is the least affected by the different
377 knockdown combinations.

378 Taken together, these data suggest that the observed effects of TRF2
379 knockdown on cell cycle progression (Figs. 3, 4 and 6) are, at least partially,
380 mediated by the reduced expression of *Cyc E*, *Cyc A* and *Cyc B* following TRF2
381 knockdown (Figs. 5 and 7d, e). Importantly, the co-occupancy of TRF2, GFZF and
382 M1BP in the promoters of these cyclin genes, the enrichment of Motif 1 in their
383 promoters and the expression patterns of the cyclin genes following the knockdown
384 of either TRF2 alone, or in combination with GFZF and/or M1BP, imply that GFZF
385 and M1BP may serve as co-factors in TRF2-regulated cell cycle progression. Yet, it
386 is TRF2 that is the major transcription factor regulating the expression pattern of the
387 abovementioned cyclin genes.

388

389 **DISCUSSION**

390 In this study, we discovered that knockdown of the general/basal transcription factor
391 TRF2 results in increased expression of the *rpr*, *hid* and *p53* pro-apoptotic genes,
392 which is in line with the observed increased apoptotic cell death following TRF2
393 knockdown and with the extensively characterized involvement of p53 in apoptosis,

394 G1 arrest and G2 arrest (reviewed, for example, in (45)). A recent study has
395 demonstrated that human TRF2 interferes with MDM2 binding and ubiquitination of
396 p53, leading to p53 protein stabilization (63). Our results provide evidence for
397 another level of p53 regulation, *i.e.*, transcriptional regulation. Furthermore, in a
398 similar manner to the p53-MDM2 negative feedback loop in vertebrates (reviewed in
399 (45)), activation of *Drosophila* p53 transcriptionally activates the *companion of reaper*
400 (*corp*) gene (64-66), which in turn, negatively regulates its activity (67). The fact that
401 *corp* expression in *Drosophila* S2R+ is rather low and not altered by TRF2
402 knockdown (Additional file 2: Table S1), may provide support for p53-independent
403 regulation of *rpr* and *hid* by TRF2.

404 Furthermore, we examined the expression of multiple additional genes
405 implicated in apoptosis following TRF2 knockdown. *Scylla* is pro-apoptotic (39) and
406 its upregulation is in line with the observed cell death following TRF2 knockdown.
407 Buffy, a *Drosophila* Bcl2 family member, however, has been shown to act in an anti-
408 apoptotic manner, but has also been shown to cause a G1-S arrest (40). Thus, its
409 upregulation following TRF2 knockdown may contribute to the observed G1-S
410 accumulation of cells. These effects are in line with studies suggesting the existence
411 of TRF2-regulated transcriptional systems (10, 16, 32, 68, 69) and are unlikely to
412 represent a general stress response, as the expression of *Debcl* and *Dronc* is not
413 affected by TRF2 knockdown.

414 Interestingly, we discovered that TRF2 knockdown results in accumulation of
415 cells in G1 and in reduction in the number of cells in S and G2/M phases. G1/S
416 transition is regulated by Cyclin E activity, while S phase and G2/M transition are
417 regulated by Cyclin A activity, and transition into and within mitosis is regulated by

418 the activities of Cyclin B and Cyclin B3. Remarkably, TRF2 knockdown in S2R+ cells
419 resulted in reduced expression of *Cyc E*, *Cyc A*, *Cyc B* and *Cyc B3* (but not *Cyc D*),
420 suggesting that TRF2 regulates cell cycle progression by modifying the expression of
421 specific cyclins. The reduced expression of *Cyc A*, *Cyc B* and *Cyc B3* and the
422 reduction of the number of cells undergoing mitosis following TRF2 knockdown, are
423 in line with previous studies, which demonstrated inhibition of nuclear mitotic entry in
424 *Drosophila* embryos following simultaneous knockdown of *Cyc A*, *Cyc B* and *Cyc B3*
425 (70). Interestingly, Cyclin A and Cyclin B have previously been shown to inhibit
426 metaphase-anaphase transition, whereas Cyclin B3 promotes it (71). Thus, the
427 specific accumulation of cells in anaphase and telophase observed by imaging flow
428 cytometry (Fig. 6e, f), could result from the reduced expression of *Cyc A* and *Cyc B*
429 following TRF2 knockdown (Fig. 5). Notably, to the best of our knowledge, this study
430 is the first to employ imaging-flow cytometry in the analysis of *Drosophila* cells.

431 To examine whether TRF2-interacting proteins could account for the observed
432 regulation of *Cyc E*, *Cyc A*, *Cyc B* and *Cyc B3* (but not *Cyc D* or *Cyc C*), we
433 searched for TRF2-interacting proteins. TRF2 has been shown to interact with M1BP
434 (57) and M1BP has been shown to interact with GFZF, a nuclear glutathione S-
435 transferase implicated in cell cycle regulation (57). Our proteomic analyses revealed
436 that both M1BP and GFZF preferentially interact with TRF2, but not with TBP (Table
437 3 and Additional file 8: Table S3). Remarkably, examination of publicly available
438 TRF2, M1BP and GFZF ChIP-exo data from *Drosophila* S2R+ cells (57, 58),
439 indicated that the effects of TRF2 knockdown on the expression of cyclin genes
440 correlate with TRF2, GFZF and M1BP co-occupancies of the promoters of the TRF2-
441 regulated cyclin genes (Table 4), in line with the reported regulatory effects of
442 GFZF. Genome-wide examination of promoters bound by all three transcription

443 factors revealed the enrichment of the TCT and Motif 1 core promoter elements.
444 Whereas one would expect the TCT to be enriched as TRF2 and M1BP have
445 previously been implicated in the regulation of ribosomal protein genes (32), the
446 enrichment of Motif 1 within promoters bound by all three factors indicates a shared
447 function for TRF2, GFZF and M1BP. Notably, in our experimental system, TRF2
448 knockdown by RNAi resulted in a two-fold reduction in *Trf2* levels (Fig. 2a, Additional
449 file 2: Table S1). Under these conditions, we did not detect any change in ribosomal
450 protein gene expression (Additional file 2: Table S1). Hence, the reduced expression
451 of *Cyc A*, *Cyc B* and *Cyc E* following a two-fold reduction in TRF2 expression, does
452 not result from a general inhibition of protein synthesis. As direct binding of TRF2 to
453 DNA could not be demonstrated (32), it is likely that TRF2 indirectly regulates the
454 expression of these cyclin genes and that there are TRF2-associated factors that
455 enable DNA binding. Our analysis suggested that GFZF and M1BP could serve as
456 such factors for specific TRF2-regulated processes. Interestingly, the expression
457 patterns of the cyclin genes following the knockdown of either TRF2 alone, or in
458 combination with GFZF and/or M1BP, indicated that among these three factors,
459 TRF2 is the major contributor to the expression pattern of *Cyc A*, *Cyc B* and *Cyc E*.
460 Moreover, while *Cyclin A*, *Cyclin B* and *Cyclin E* expression levels are reduced
461 following TRF2 (but not GFZF) knockdown, the expression levels of both *Cyclin A*
462 and *Cyclin B* , but not *Cyclin E*, are reduced following the combined knockdown of
463 TRF2 and GFZF (Fig. 7d, e), suggesting that the reduced expression levels of *Cyclin*
464 *A* and *Cyclin B* are not mediated via *Cyclin E*.

465 Notably, mouse TBP was recently shown to remain bound to mitotic
466 chromosomes during mitosis of mouse embryonic stem cells (mESCs), and to recruit
467 a small population of Pol II molecules to mitotic chromosomes (72). Nevertheless,

468 active Pol II transcription occurs in the absence of mouse TBP, whereas Pol I and
469 Pol III, are significantly reduced (11, 72). It remains to be determined whether
470 *Drosophila* TBP is bound to mitotic chromosomes during mitosis. As we did not
471 observe significant effects on cell cycle progression or mitosis following *Drosophila*
472 TBP knockdown (Figs. 3, 4 and 6), it is likely that *mouse* TBP may exert different
473 functions as compared to *Drosophila* TBP, perhaps via its associated proteins.

474 The effects of TRF2 knockdown on cell cycle progression and apoptosis of
475 *Drosophila* cultured S2R+ cells are in line with the early embryonic lethality of TRF2
476 knockout flies. TRF2 has also been shown to be essential for embryonic
477 development of *C. elegans*, zebrafish and *Xenopus*. It remains to be determined
478 whether knockdown of TRF2 in cellular systems from these species results in similar
479 effects.

480 **CONCLUSIONS**

481 Taken together, using *Drosophila* cells as a model system, we discovered that the
482 knockdown of TRF2, rather than TBP or TRF1, regulates apoptosis and cell cycle
483 progression via distinct target genes. Importantly, we discovered that TRF2 is
484 associated with the GFZF and M1BP proteins, and that TRF2, GFZF and M1BP co-
485 occupy the promoters of the TRF2-regulated cyclins. Furthermore, we show that
486 TRF2, rather than GFZF or M1BP, is the major contributor to the expression pattern
487 of *Cyc E*, *Cyc A* and *Cyc B*. Importantly, while a general transcription factor may be
488 regarded as having a “generic function”, our findings emphasize the unique,
489 unanticipated functions of *Drosophila* TRF2 as an essential factor for specific major
490 cellular processes.

491 # MATERIALS AND METHODS

492

493 ***Drosophila melanogaster* Schneider S2R+ Cells**

494 *Drosophila melanogaster* Schneider S2R+ adherent cells were cultured in

495 Schneider's *Drosophila* Media (Biological Industries) that was supplemented with

496 10% heat-inactivated FBS and Penicillin 100 units/ml Streptomycin 0.1mg/ml

497 (Biological Industries).

498

499 **Generation of dsRNA probes**

500 All dsRNA probes were chosen based on http://www.dkfz.de/signaling/e-rnai3// and

501 http://www.flyrnai.org/snapdragon as described in (69). Primer sequences used for

502 the generation of dsRNA probes are provided in Table 1. DNA fragments

503 corresponding to each dsRNA were subcloned into both pBlueScript SK+ and KS+.

504 The dsRNA probes were generated by PCR amplification of the DNA using T7 and

505 T3 primers, followed by *in vitro* transcription of templates in both pBlueScript

506 orientations using T7 RNA polymerase. Resulting RNA products were annealed to

507 generate the dsRNA probes.

508

509 **RNA interference (RNAi)**

510 For 6 well plate, $1.25x10^6$ cells/well were resuspended and seeded in empty

511 Schneider's *Drosophila* Media (Biological Industries) with 30µg/ml dsRNA directed

512 against different genes for 1 hour. Next, two volumes of complete medium were

513 added to the wells and cells were incubated for 3 additional days.

514

515

516

517 **Western blot analysis**

518 Knockdown of TRF2 and TBP was verified by western blot analysis using anti-TRF2
519 and anti-TBP polyclonal antibodies (generous gift from Jim Kadonaga). Cyclin E
520 levels were analyzed by the 8B10 antibodies (generous gift from Helena Richardson)
521 (73). The levels of Actin or γ-Tubulin, as a loading control, were detected using either
522 mouse monoclonal anti-Actin (Abcam, 8224) or anti- γ-Tubulin (Sigma, GTU-88)
523 antibodies. Anti-Cyclin A and -Cyclin B concentrated monoclonal antibodies
524 (Developmental Studies Hybridoma Bank, A12 and F2F4, respectively) were tested
525 as well, however no endogenous proteins were detected, possibly due to technical
526 limitations.

527

528 **TBP expression vector**

529 The coding sequence of *Drosophila* TBP was amplified by PCR and cloned with an
530 N-terminal Flag-HA tag into the pAc5.1 vector (Life Technologies) using cDNA from
531 S2R+ cells as template and the following primers: Forward (containing an XhoI site,
532 underlined)
533 5' CCGCTCGAGGACCAAATGCTAAGCCCCA 3' and reverse (containing an AgeI
534 site, underlined) 5' AGCACCGGTTTATGACTGCTTCTTGAACTTCTTTAA 3'
535 Plasmid sequence was verified by sequencing.

536 **RNAi-coupled overexpression**

537 For 6 well plate, 1.25×10^6 *Drosophila* S2R+ cells/well were resuspended and seeded
538 in empty medium with 30µg/ml dsRNA directed against TRF2 for 1 hour. Next, two
539 volumes of complete medium were added to the wells and cells were incubated for 3
540 days. Three days post dsRNA treatment, cells were transfected with the TBP-pAc
541 expression vector (930 ng) or an empty vector control using the Escort IV reagent

542 (Sigma). Media was replaced 18-24 hrs post transfection. Cells were harvested 36-
543 48 hrs post transfection and RNA was purified and analyzed by RT-qPCR. Each
544 qPCR experiment was performed in triplicates. The graphs represent an average of
545 3 independent experiments. Error bars represent SEM.
546
547 **RNA-seq analysis**
548 S2R+ cells were treated with dsRNA probes against *Trf2* (probe #1) and *Tbp*, and
549 harvested at two time points - 48h and 72h post RNAi treatment. For each time point,
550 a matched mock control was collected separately.
551 RNA was extracted using Quick-RNA™ MiniPrep (Zymo Research), and 800ng of
552 each sample was purified using NEBNext Poly(A) mRNA Magnetic Isolation Module
553 (NEB #E7490). Libraries were prepared using NEBNext Ultra II RNA Library Prep Kit
554 for Illumina (NEB #E7770), following the manufacturer's instructions. NEBNext
555 Multiplex Oligos for Illumina (NEB #E7335, NEB #E7500, NEB #E7710, NEB
556 #E7730) were used. Libraries were pooled and a 1% PhiX library control was added.
557 Single-end sequencing was performed on an Illumina NextSeq 500 machine.
558 Reads were aligned to dm6 genome build using STAR (version 2.6.0a), and htseq-
559 count (version 0.5.1p3, (74)) was used to count the reads mapped to each gene.
560 Differential expression analysis of conditions was performed using the DESeq2 R
561 package (75). Only genes with adjusted p-value < 0.1 were considered for
562 subsequent analysis. GO terms analysis was carried out using STRING v11 (76).
563 For all experiments, three independent biological replicates were compared and
564 merged for subsequent analysis. RNA-seq Data is available at GSE133685.
565
566

567 **RT-PCR**

568 Total RNA was isolated using the PerfectPure RNA Cultured Cell kit (5 PRIME) or
569 Quick-RNA^{TM} MiniPrep (Zymo Research). One microgram of the total RNA was
570 reverse-transcribed into cDNA with M-MLV (Promega) or qScript Flex cDNA Kit
571 (Quanta). Control reactions lacking reverse transcriptase were also performed to
572 ensure that the levels of contaminating genomic DNA were negligible. Quantitation
573 was performed by real-time PCR to determine the transcription levels of the
574 endogenous genes. The expression levels were compared to *Gapdh2*. Primer
575 sequences for real-time PCR are provided in Table 2. For all quantifications, the
576 error bars represent ±S.E.M of at least 3 independent experiments; NS, not
577 significant; $^{**}P < 0.01$; $^{***}P < 0.001$. Statistical analyses were performed on log-
578 transformed relative quantification (RQ) values using one-way ANOVA followed by
579 Tukey's post hoc test, unless otherwise stated in the figure legend.

580

581 **Flow cytometry analysis**

582 For cell cycle distribution by Propidium Iodide (PI) staining, cells were harvested
583 following 72h incubation with dsRNA, centrifuged for 5 min at 300g and fixed with
584 80% ethanol at 4ºC overnight. Before subjecting the cells to flow cytometry, the cells
585 were centrifuged for 5 min at 300g, washed in 1 ml of Phosphate-buffered saline
586 (PBS) and incubated for 40 min at 4°C. The cells were then stained in PBS
587 containing 50 µg/ml PI (Sigma) and 50 µg/ml RNase A (Roche). After incubation for
588 15 min at room temperature, fluorescence was measured using a FACSCalibur
589 Becton Dickinson flow cytometer.

590 For analyzing apoptosis by Annexin V and PI staining, cells were harvested 72h
591 following incubation with dsRNA probes and stained with Annexin V and PI

592 (MEBCYTO Apoptosis Kit; MBL). Fluorescence was measured using a FACSCalibur
593 Becton Dickinson flow cytometer.
594 For G1 phase cell arrest by hydroxyurea (HU) and BrdU (5-Bromo-2´-Deoxyuridine)-
595 PI staining, 72h following incubation with dsRNA, the medium was replaced with
596 medium containing a final concentration of 1mM HU for 18h (77) (for control cells,
597 the medium was replaced with a fresh medium). BrdU (40μM final concentration)
598 was added to the medium for 2h. Cells were released from HU by medium
599 replacement and, at 0, 2, 4, 6 or 8 hours following the release, cells were harvested,
600 centrifuged and fixed with 80% ethanol at 4ºC overnight. Following fixation, cells
601 were stained with FITC *(Fluorescein isothiocyanate)*-conjugated anti-Brdu antibodies
602 (BD) and PI according to the provided protocol, and fluorescence was measured
603 using BD FACSARIA III. All flow cytometry data was analyzed using the FlowJo
604 software. Statistical analyses of flow cytometry and imaging flow cytometry data
605 were performed in SPSS using two-tailed Students t-test. The number of times each
606 experiment was repeated, is detailed in the figure legends.
607 It is of note that unfortunately, we were unable to synchronize cells in G2/M in
608 a reversible manner using either Nocodazole or Colchicine, which cause
609 microtubules depolymerization. Specifically, Nocadazole did not arrest the S2R+
610 cells in G2/M, while Colchicine, which has been used since the 1950s to inhibit
611 mitotic progression, did cause enrichment of mitotic cells (Fig. 6b, d). However, this
612 effect was irreversible (data not shown). Thus, Colchicine could not be used for
613 G2/M block-release synchronization experiments.
614
615

616 **Immunostaining for fluorescence microscopy and Imaging flow cytometry**
617 **analysis**
618 Cells were RNAi-treated as described above. On day 4, 2ml of fresh medium was
619 added to the wells. To enrich for G2/M, as a control, Colchicine (Sigma) was added
620 to a final concentration of 350ng/ml. On the following day, the cells were harvested
621 and fixed with 4% Paraformaldehyde (PFA)/PBS (30 min), washed in PBST (PBS
622 containing 0.5% Triton x), blocked with PBS containing 1% BSA and 1% serum (1h),
623 and incubated with phospho-Histone H3 (Ser10) antibody (1:200, Cell Signaling
624 Technology #9701) for 1h at RT, followed by overnight at 4°C. Cells were washed,
625 stained with the secondary antibody (1:500, DyLight 488, ab96883), and then
626 counter-stained with 10µg/ml Hoechst 33342 (Sigma). For microscopy analysis,
627 samples were also stained for filamentous Actin with 3.5µM Acti-stain 670 Phalloidin
628 (Cytoskeleton, Inc. Cat. # PHDN1). Following staining, samples were subjected to
629 imaging flow cytometry, confocal microscopy or wide-field fluorescence microscopy
630 analysis.
631
632 **Microscope image analyses**
633 High resolution images were acquired using a Leica SP8 confocal microscope, and
634 high-throughput images for quantitative analysis were acquired using a Leica DMi8
635 microscope. Three separate experiments were performed and captured at 20x
636 magnification. For each treatment, approximately 275 frames were acquired and
637 analysed. The total number of Alexa 488 anti-phosphor-Histone H3 (Ser10) (PH3)
638 labeled cells, and the total number of Hoechst stained cells, were calculated using
639 the Fiji distribution of ImageJ.
640 Analysis workflow:

641 1. The raw PH3 channel images were enhanced using brightness and contrast, and
642 then the background was subtracted by reducing the Gaussian blurred filtered
643 image of the enhanced image. Next, a median filter was applied to smoothen the
644 image and an Otsu threshold was applied to get the binary image of all mitotic
645 nuclei. Finally, watershed was implemented to separate touching nuclei. Mitotic
646 cells were counted, eliminating small debris and noise.
647 2. To analyze the Hoechst channel, the background was subtracted by reducing the
648 Gaussian blurred filtered image of the original image. Next, a Moments threshold
649 was applied to get the binary image of total nuclei. Finally, watershed was
650 implemented to separate touching nuclei. Nuclei were counted while eliminating
651 small debris and noise.

652 The ratio between the number of mitotic cells and the total number of cells yields the
653 mitotic index for each treatment.
654 All manipulations in the images were made evenly across the entire field.
655 The Fiji macros will be shared upon request.
656

657 **Multispectral imaging flow-cytometry (IFC) analysis**

658 Cells were imaged using multispectral imaging flow cytometry (ImageStreamX mark
659 II imaging flow-cytometer; Amnis Corp, Seattle, WA, Part of EMD Millipore). Each
660 experiment was performed 3 times. In each experiment, at least 40,000 cells were
661 collected from each sample, and data were analyzed using the image analysis
662 software (IDEAS 6.2; Amnis Corp). Images were compensated for fluorescent dye
663 overlap by using single-stain controls. Imaging flow cytometry results were analyzed
664 by calculation of a set of parameters, termed “features”, performed on a defined area
665 of interest, termed “mask”. The serial gating strategy to identify the mitotic cell

666 population was as follows: Single cells were first gated using the area and aspect
667 ratio features on the bright-field (BF) image (the aspect ratio, which indicates how
668 round or oblong an object is, is calculated by division of the minor axis by the major
669 axis). Uncropped cells were gated using the centroid X (the number of pixels in the
670 horizontal axis from the upper left corner of the image to the center of the mask) and
671 area features. Focused cells were gated using the Gradient RMS feature, as
672 previously described (78) (Additional file 5: Figure S4a-c). Following this standard
673 gating series, the mitotic cell fraction of the entire cell population was identified using
674 the staining intensity for PH3 AF488 (channel 2), and mitotic cells were gated as the
675 high intensity population of PH3 staining within all focused cells (Additional file 5:
676 Figure S4d,e).
677 For a more complex analysis, we performed a second gating series. Focused cells
678 were first gated for G2/M based on DNA (Hoechst) intensity (Additional file 5: Figure
679 S4) and then gated for mitotic cells, as previously, by high PH3 intensity. To further
680 subdivide into the specific cell division phases, we gated according to nuclear
681 morphology based on the spot count and aspect ratio intensity features (see
682 Additional file 5: Figure S4f, g for detailed masking and gating). As it was previously
683 shown that serine 10 of histone H3 becomes dephosphorylated during telophase
684 (79), the telophase population was derived from the negative PH3-stained cells,
685 based on the BF circularity feature and DNA aspect ratio intensity (see Additional file
686 5: Figure S4h for detailed masking and gating). Full details of all masking, features
687 and analysis strategies are included in the legend of Additional file 5: Figure S4.

688 **Identification of unique TRF2-interacting proteins**

689 To identify the proteins that are in complex with TRF2 (the evolutionarily conserved
690 short TRF2), we used inducible FLAG-HA-tagged TRF2 S2R+ cells (69). As

691 controls, we used inducible S2R+ for FLAG-HA-long TRF2 (69) or FLAG-HA-TBP
692 (generated as in (69)). Cells were either induced by copper sulfate or left untreated.
693 Protein extracts were prepared and TRF2-containing complexes were immuno-
694 precipitated using anti-FLAG M2 affinity gel (Sigma). Following the IP, TRF2-
695 containing complexes were released with a FLAG peptide (Sigma). Samples were
696 resolved by SDS-PAGE. Proteins that were purified from TRF2-induced cells were
697 separated to two samples: proteins larger or smaller than 40 kDa. Samples were
698 subjected to Mass spectrometry analyses (The Smoler Protein Research Center,
699 Technion). Briefly, samples were digested by trypsin, analyzed by LC-MS/MS on Q-
700 Exactive Plus (ThermoFisher) and identified by the Discoverer software (with two
701 search algorithms: Sequest (ThermoFisher) and Mascot (Matrix science) against the
702 *Drosophila melanogaster* section of the NCBI non-redundant and Uniprot databases,
703 and a decoy database (in order to determine the false discovery rate). All the
704 identified peptides were filtered with high confidence, top rank, mass accuracy, and a
705 minimum of 2 peptides. High confidence peptides have passed the 1% FDR
706 threshold. Semi-quantitation was done by calculating the peak area of each peptide.
707 The area of the protein is the average of the three most intense peptides from each
708 protein. The results are provided in Additional file 8: Table S3.

709

710 **Visualization of publicly available ChIP-exo data**

711 A genome browser session
712 (https://genome.ucsc.edu/s/Anna%20Sloutskin/dm3_ChIP_Exo) based on available
713 TRF2, GFZF and M1BP ChIP-exo bedgraph files (GSE97841, GSE105009) (57, 58)
714 was created. The session contains an “Overlap” track (the ChIP-exo peaks that were
715 identified as overlapping in the ±50bp window relative to FlyBase TSS) and the

716 “trustedTSS” track that is based on 5’ GRO-seq (GSE68677) and PRO-Cap

717 (GSM1032759) data. The relevant interval (±50bp or 100bp) is indicated.

718

719 **List of abbreviations**

720 ChIP-exo - chromatin immunoprecipitation combined with exonuclease digestion

721 followed by high-throughput sequencing

722 DPE - downstream core promoter element

723 GFZF - GST-containing FLYWCH zinc-finger protein

724 M1BP - Motif 1 binding protein

725 Pol II - RNA polymerase II

726 TBP - TATA-box-binding protein

727 TRF2 - TBP-related factor 2

728 TSS - Transcription start site

729

730

731 **Declarations**

732 **Ethics approval and consent to participate**

733 Not applicable

734

735 **Consent for publication**

736 Not applicable

737

738 **Availability of data and materials**

739 RNAseq data generated during the current study is available in the GEO repository

740 (GSE133685).

741 ChIP-exo data analyzed during the current study was downloaded from the GEO
742 (GSE97841, GSE105009).
743
744 **Competing interests**
745 The authors declare that they have no competing interests
746
747 **Funding**
748 This work was supported by grants from the Israel Science Foundation to T.J.-G.
749 (no. 798/10 and no. 1234/17).
750
751 **Authors' contributions**
752 A. Kedmi prepared RNA samples and O. Yaron and A. Sloutskin performed RNA-
753 seq experiments. T. Doniger and A. Sloutskin analyzed the RNA-seq experiments
754 and performed bioinformatics analysis. A. Kedmi, N. Epstein, L. Gasri-Plotnitsky and
755 D. Ickowicz performed and/or analyzed flow cytometry experiments. A. Kedmi, A.
756 Sloutskin and D. Ideses performed reverse transcription-qPCR analysis. I. Shoval
757 and Z. Porat advised and performed the analysis of ImageStream® experiments, A.
758 Kedmi and I. Shoval performed and analyzed fluorescence microscopy experiments.
759 E. Darmon and D. Ideses performed western blot analyses. A. Sloutskin performed
760 the statistical analysis. A. Kedmi, A. Sloutskin and T. Juven-Gershon designed the
761 study, planned experiments, analyzed results, and wrote the manuscript with input
762 from all authors.
763
764
765

766 **Acknowledgements**

767 We thank Jim Kadonaga for the generous gift of anti-TRF2 and anti-TBP antibodies,
768 for invaluable advice and assistance and for critical reading of the manuscript. We
769 thank Helena Richardson for the generous gift of anti-Cyclin E antibodies. We thank
770 Moshe Oren, Doron Ginsberg, Ze'ev Paroush, Sivan Henis-Korenblit, Shaked Cohen
771 and Itay Lazar for invaluable advice and assistance. We thank Dr. Jennifer Israel-
772 Cohen for assistance with statistical analysis. We thank Doron Ginsberg, Yaron
773 Shav-Tal, Galit Shohat-Ophir and Orit Adato for critical reading of the manuscript.
774 We thank Orit Adato and Sarit Lampert for technical assistance.

775

776 **REFERENCES**

777 1. Danino YM, Even D, Ideses D, Juven-Gershon T. The core promoter: At the
778 heart of gene expression. Biochimica et biophysica acta. 2015;1849(8):1116-31.
779 2. Goodrich JA, Tjian R. Unexpected roles for core promoter recognition factors in
780 cell-type-specific transcription and gene regulation. Nature reviews Genetics.
781 2010;11(8):549-58.
782 3. Muller F, Tora L. Chromatin and DNA sequences in defining promoters for
783 transcription initiation. Biochimica et biophysica acta. 2014;1839(3):118-28.
784 4. Thomas MC, Chiang CM. The general transcription machinery and general
785 cofactors. Crit Rev Biochem Mol Biol. 2006;41(3):105-78.
786 5. Dikstein R. The unexpected traits associated with core promoter elements.
787 Transcription. 2011;2(5):201-6.
788 6. Haberle V, Stark A. Eukaryotic core promoters and the functional basis of
789 transcription initiation. Nature reviews Molecular cell biology. 2018;19(10):621-
790 37.
791 7. Kadonaga JT. Perspectives on the RNA polymerase II core promoter. Wiley
792 Interdiscip Rev Dev Biol. 2012;1(1):40-51.
793 8. Lenhard B, Sandelin A, Carninci P. Metazoan promoters: emerging
794 characteristics and insights into transcriptional regulation. Nature reviews
795 Genetics. 2012;13(4):233-45.
796 9. Ohler U, Wassarman DA. Promoting developmental transcription. Development.
797 2010;137(1):15-26.
798 10. Vo Ngoc L, Wang YL, Kassavetis GA, Kadonaga JT. The punctilious RNA
799 polymerase II core promoter. Genes & development. 2017;31(13):1289-301.
800 11. Martianov I, Viville S, Davidson I. RNA polymerase II transcription in murine cells
801 lacking the TATA binding protein. Science. 2002;298(5595):1036-9.
802 12. Akhtar W, Veenstra GJ. TBP-related factors: a paradigm of diversity in
803 transcription initiation. Cell & bioscience. 2011;1(1):23.
804 13. Muller F, Zaucker A, Tora L. Developmental regulation of transcription initiation:
805 more than just changing the actors. Current opinion in genetics & development.
806 2010;20(5):533-40.
807 14. Reina JH, Hernandez N. On a roll for new TRF targets. Genes & development.
808 2007;21(22):2855-60.
809 15. Torres-Padilla ME, Tora L. TBP homologues in embryo transcription: who does
810 what? EMBO reports. 2007;8(11):1016-8.
811 16. Zehavi Y, Kedmi A, Ideses D, Juven-Gershon T. TRF2: TRansForming the view
812 of general transcription factors. Transcription. 2015:0.
813 17. Hansen SK, Takada S, Jacobson RH, Lis JT, Tjian R. Transcription properties of
814 a cell type-specific TATA-binding protein, TRF. Cell. 1997;91(1):71-83.
815 18. Dantonel JC, Wurtz JM, Poch O, Moras D, Tora L. The TBP-like factor: an
816 alternative transcription factor in metazoa? Trends in biochemical sciences.
817 1999;24(9):335-9.
818 19. Duttke SH, Doolittle RF, Wang YL, Kadonaga JT. TRF2 and the evolution of the
819 bilateria. Genes & development. 2014;28(19):2071-6.
820 20. Moore PA, Ozer J, Salunek M, Jan G, Zerby D, Campbell S, et al. A human
821 TATA binding protein-related protein with altered DNA binding specificity inhibits
822 transcription from multiple promoters and activators. Molecular and cellular
823 biology. 1999;19(11):7610-20.

21. Persengiev SP, Zhu X, Dixit BL, Maston GA, Kittler EL, Green MR. TRF3, a TATA-box-binding protein-related factor, is vertebrate-specific and widely expressed. Proceedings of the National Academy of Sciences of the United States of America. 2003;100(25):14887-91.
22. Rabenstein MD, Zhou S, Lis JT, Tjian R. TATA box-binding protein (TBP)-related factor 2 (TRF2), a third member of the TBP family. Proceedings of the National Academy of Sciences of the United States of America. 1999;96(9):4791-6.
23. Kopytova DV, Krasnov AN, Kopantceva MR, Nabirochkina EN, Nikolenko JV, Maksimenko O, et al. Two isoforms of Drosophila TRF2 are involved in embryonic development, premeiotic chromatin condensation, and proper differentiation of germ cells of both sexes. Molecular and cellular biology. 2006;26(20):7492-505.
24. Bashirullah A, Lam G, Yin VP, Thummel CS. dTrf2 is required for transcriptional and developmental responses to ecdysone during Drosophila metamorphosis. Developmental dynamics : an official publication of the American Association of Anatomists. 2007;236(11):3173-9.
25. Dantonel JC, Quintin S, Lakatos L, Labouesse M, Tora L. TBP-like factor is required for embryonic RNA polymerase II transcription in C. elegans. Molecular cell. 2000;6(3):715-22.
26. Jacobi UG, Akkers RC, Pierson ES, Weeks DL, Dagle JM, Veenstra GJ. TBP paralogs accommodate metazoan- and vertebrate-specific developmental gene regulation. The EMBO journal. 2007;26(17):3900-9.
27. Kaltenbach L, Horner MA, Rothman JH, Mango SE. The TBP-like factor CeTLF is required to activate RNA polymerase II transcription during C. elegans embryogenesis. Molecular cell. 2000;6(3):705-13.
28. Levine M, Cattoglio C, Tjian R. Looping back to leap forward: transcription enters a new era. Cell. 2014;157(1):13-25.
29. Muller F, Lakatos L, Dantonel J, Strahle U, Tora L. TBP is not universally required for zygotic RNA polymerase II transcription in zebrafish. Current biology : CB. 2001;11(4):282-7.
30. Neves A, Eisenman RN. Distinct gene-selective roles for a network of core promoter factors in Drosophila neural stem cell identity. Biology open. 2019;8(4).
31. Veenstra GJ, Weeks DL, Wolffe AP. Distinct roles for TBP and TBP-like factor in early embryonic gene transcription in Xenopus. Science. 2000;290(5500):2312-5.
32. Wang YL, Duttke SH, Chen K, Johnston J, Kassavetis GA, Zeitlinger J, et al. TRF2, but not TBP, mediates the transcription of ribosomal protein genes. Genes & development. 2014;28(14):1550-5.
33. Martianov I, Fimia GM, Dierich A, Parvinen M, Sassone-Corsi P, Davidson I. Late arrest of spermiogenesis and germ cell apoptosis in mice lacking the TBP-like TLF/TRF2 gene. Molecular cell. 2001;7(3):509-15.
34. Zhang D, Penttila TL, Morris PL, Roeder RG. Cell- and stage-specific high-level expression of TBP-related factor 2 (TRF2) during mouse spermatogenesis. Mechanisms of development. 2001;106(1-2):203-5.
35. Zhang D, Penttila TL, Morris PL, Teichmann M, Roeder RG. Spermiogenesis deficiency in mice lacking the Trf2 gene. Science. 2001;292(5519):1153-5.
36. Deveraux QL, Reed JC. IAP family proteins--suppressors of apoptosis. Genes & development. 1999;13(3):239-52.

872 37. Fuchs Y, Steller H. Live to die another way: modes of programmed cell death
873 and the signals emanating from dying cells. Nature reviews Molecular cell
874 biology. 2015;16(6):329-44.
875 38. Martin SJ. Destabilizing influences in apoptosis: sowing the seeds of IAP
876 destruction. Cell. 2002;109(7):793-6.
877 39. Scuderi A, Simin K, Kazuko SG, Metherall JE, Letsou A. scylla and charybde,
878 homologues of the human apoptotic gene RTP801, are required for head
879 involution in Drosophila. Dev Biol. 2006;291(1):110-22.
880 40. Quinn L, Coombe M, Mills K, Daish T, Colussi P, Kumar S, et al. Buffy, a
881 Drosophila Bcl-2 protein, has anti-apoptotic and cell cycle inhibitory functions.
882 The EMBO journal. 2003;22(14):3568-79.
883 41. Brachmann CB, Jassim OW, Wachsmuth BD, Cagan RL. The Drosophila bcl-2
884 family member dBorg-1 functions in the apoptotic response to UV-irradiation.
885 Current biology : CB. 2000;10(9):547-50.
886 42. Colussi PA, Quinn LM, Huang DC, Coombe M, Read SH, Richardson H, et al.
887 Debcl, a proapoptotic Bcl-2 homologue, is a component of the Drosophila
888 melanogaster cell death machinery. The Journal of cell biology.
889 2000;148(4):703-14.
890 43. Igaki T, Kanuka H, Inohara N, Sawamoto K, Nunez G, Okano H, et al. Drob-1, a
891 Drosophila member of the Bcl-2/CED-9 family that promotes cell death.
892 Proceedings of the National Academy of Sciences of the United States of
893 America. 2000;97(2):662-7.
894 44. Zhang H, Huang Q, Ke N, Matsuyama S, Hammock B, Godzik A, et al.
895 Drosophila pro-apoptotic Bcl-2/Bax homologue reveals evolutionary conservation
896 of cell death mechanisms. The Journal of biological chemistry.
897 2000;275(35):27303-6.
898 45. Levine AJ, Oren M. The first 30 years of p53: growing ever more complex. Nat
899 Rev Cancer. 2009;9(10):749-58.
900 46. Vousden KH, Lane DP. p53 in health and disease. Nature reviews Molecular cell
901 biology. 2007;8(4):275-83.
902 47. Brodsky MH, Nordstrom W, Tsang G, Kwan E, Rubin GM, Abrams JM.
903 Drosophila p53 binds a damage response element at the reaper locus. Cell.
904 2000;101(1):103-13.
905 48. Fan Y, Lee TV, Xu D, Chen Z, Lamblin AF, Steller H, et al. Dual roles of
906 Drosophila p53 in cell death and cell differentiation. Cell Death Differ.
907 2010;17(6):912-21.
908 49. Teichmann M, Wang Z, Martinez E, Tjernberg A, Zhang D, Vollmer F, et al.
909 Human TATA-binding protein-related factor-2 (hTRF2) stably associates with
910 hTFIIA in HeLa cells. Proceedings of the National Academy of Sciences of the
911 United States of America. 1999;96(24):13720-5.
912 50. Baldin V, Lukas J, Marcote MJ, Pagano M, Draetta G. Cyclin D1 is a nuclear
913 protein required for cell cycle progression in G1. Genes & development.
914 1993;7(5):812-21.
915 51. Matsushime H, Roussel MF, Ashmun RA, Sherr CJ. Colony-stimulating factor 1
916 regulates novel cyclins during the G1 phase of the cell cycle. Cell.
917 1991;65(4):701-13.
918 52. Dulic V, Lees E, Reed SI. Association of human cyclin E with a periodic G1-S
919 phase protein kinase. Science. 1992;257(5078):1958-61.

920 53. Koff A, Giordano A, Desai D, Yamashita K, Harper JW, Elledge S, et al.
921 Formation and activation of a cyclin E-cdk2 complex during the G1 phase of the
922 human cell cycle. Science. 1992;257(5077):1689-94.
923 54. Taylor EW. The Mechanism of Colchicine Inhibition of Mitosis. I. Kinetics of
924 Inhibition and the Binding of H3-Colchicine. The Journal of cell biology.
925 1965;25:SUPPL:145-60.
926 55. Hervás JP, Fernández-Gómez ME, Giménez-Martín G. Colchicine Effect on the
927 Mitotic Spindle: Estimate of Multipolar Anaphase Production. Caryologia.
928 1974;27(3):359-68.
929 56. Rieder CL, Palazzo RE. Colcemid and the mitotic cycle. Journal of cell science.
930 1992;102 (Pt 3):387-92.
931 57. Baumann DG, Gilmour DS. A sequence-specific core promoter-binding
932 transcription factor recruits TRF2 to coordinately transcribe ribosomal protein
933 genes. Nucleic acids research. 2017;45(18):10481-91.
934 58. Baumann DG, Dai MS, Lu H, Gilmour DS. GFZF, a glutathione S-transferase
935 protein implicated in cell cycle regulation and hybrid inviability, is a transcriptional
936 co-activator. Molecular and cellular biology. 2017.
937 59. Bailey TL, Boden M, Buske FA, Frith M, Grant CE, Clementi L, et al. MEME
938 SUITE: tools for motif discovery and searching. Nucleic acids research.
939 2009;37(Web Server issue):W202-8.
940 60. Ohler U, Liao GC, Niemann H, Rubin GM. Computational analysis of core
941 promoters in the Drosophila genome. Genome Biol.
942 2002;3(12):RESEARCH0087.
943 61. Sloutskin A, Danino YM, Orenstein Y, Zehavi Y, Doniger T, Shamir R, et al.
944 ElemeNT: a computational tool for detecting core promoter elements.
945 Transcription. 2015;6(3):41-50.
946 62. Li J, Gilmour DS. Distinct mechanisms of transcriptional pausing orchestrated by
947 GAGA factor and M1BP, a novel transcription factor. The EMBO journal.
948 2013;32(13):1829-41.
949 63. Maeda R, Tamashiro H, Takano K, Takahashi H, Suzuki H, Saito S, et al. TBP-
950 like Protein (TLP) Disrupts the p53-MDM2 Interaction and Induces Long-lasting
951 p53 Activation. The Journal of biological chemistry. 2017;292(8):3201-12.
952 64. Akdemir F, Christich A, Sogame N, Chapo J, Abrams JM. p53 directs focused
953 genomic responses in Drosophila. Oncogene. 2007;26(36):5184-93.
954 65. Brodsky MH, Weinert BT, Tsang G, Rong YS, McGinnis NM, Golic KG, et al.
955 Drosophila melanogaster MNK/Chk2 and p53 regulate multiple DNA repair and
956 apoptotic pathways following DNA damage. Molecular and cellular biology.
957 2004;24(3):1219-31.
958 66. Zhang Y, Lin N, Carroll PM, Chan G, Guan B, Xiao H, et al. Epigenetic blocking
959 of an enhancer region controls irradiation-induced proapoptotic gene expression
960 in Drosophila embryos. Developmental cell. 2008;14(4):481-93.
961 67. Chakraborty R, Li Y, Zhou L, Golic KG. Corp Regulates P53 in Drosophila
962 melanogaster via a Negative Feedback Loop. PLoS Genet.
963 2015;11(7):e1005400.
964 68. Isogai Y, Keles S, Prestel M, Hochheimer A, Tjian R. Transcription of histone
965 gene cluster by differential core-promoter factors. Genes & development.
966 2007;21(22):2936-49.
967 69. Kedmi A, Zehavi Y, Glick Y, Orenstein Y, Ideses D, Wachtel C, et al. Drosophila
968 TRF2 is a preferential core promoter regulator. Genes & development.
969 2014;28(19):2163-74.

970 70. McCleland ML, O'Farrell PH. RNAi of mitotic cyclins in Drosophila uncouples the
971 nuclear and centrosome cycle. Current biology : CB. 2008;18(4):245-54.
972 71. Yuan K, O'Farrell PH. Cyclin B3 is a mitotic cyclin that promotes the metaphase-
973 anaphase transition. Current biology : CB. 2015;25(6):811-6.
974 72. Teves SS, An L, Bhargava-Shah A, Xie L, Darzacq X, Tjian R. A stable mode of
975 bookmarking by TBP recruits RNA polymerase II to mitotic chromosomes. eLife.
976 2018;7:e35621.
977 73. Richardson H, O'Keefe LV, Marty T, Saint R. Ectopic cyclin E expression
978 induces premature entry into S phase and disrupts pattern formation in the
979 Drosophila eye imaginal disc. Development. 1995;121(10):3371-9.
980 74. Anders S, Pyl PT, Huber W. HTSeq--a Python framework to work with high-
981 throughput sequencing data. Bioinformatics. 2015;31(2):166-9.
982 75. Love MI, Huber W, Anders S. Moderated estimation of fold change and
983 dispersion for RNA-seq data with DESeq2. Genome Biol. 2014;15(12):550.
984 76. Szklarczyk D, Gable AL, Lyon D, Junge A, Wyder S, Huerta-Cepas J, et al.
985 STRING v11: protein-protein association networks with increased coverage,
986 supporting functional discovery in genome-wide experimental datasets. Nucleic
987 acids research. 2019;47(D1):D607-D13.
988 77. Peng Q, Wang Y, Li M, Yuan D, Xu M, Li C, et al. cGMP-Dependent Protein
989 Kinase Encoded by foraging Regulates Motor Axon Guidance in Drosophila by
990 Suppressing Lola Function. J Neurosci. 2016;36(16):4635-46.
991 78. George TC, Fanning SL, Fitzgerald-Bocarsly P, Medeiros RB, Highfill S, Shimizu
992 Y, et al. Quantitative measurement of nuclear translocation events using
993 similarity analysis of multispectral cellular images obtained in flow. J Immunol
994 Methods. 2006;311(1-2):117-29.
995 79. Hendzel MJ, Wei Y, Mancini MA, Van Hooser A, Ranalli T, Brinkley BR, et al.
996 Mitosis-specific phosphorylation of histone H3 initiates primarily within
997 pericentromeric heterochromatin during G2 and spreads in an ordered fashion
998 coincident with mitotic chromosome condensation. Chromosoma.
999 1997;106(6):348-60.
1000 80. Filby A, Perucha E, Summers H, Rees P, Chana P, Heck S, et al. An imaging
1001 flow cytometric method for measuring cell division history and molecular
1002 symmetry during mitosis. Cytometry A. 2011;79(7):496-506.
1003

1004 ## Figure Legends

1005 **Fig. 1.**

1006 *Trf2* Knockdown enhances early and late apoptosis in S2R+ cells. *Drosophila* S2R+
1007 cells were incubated for three days with dsRNA directed against *Trf2*, *exd*, *Tbp* and
1008 *Trf1*. To examine whether *Trf2* knockdown triggers apoptotic cell death, cells were
1009 harvested following 72 h and stained with Annexin-V FITC and PI. **a** FACS analysis
1010 of a representative experiment. **b** Average percentages of cells undergoing early and
1011 late apoptosis. (n=4, *$0.01 < p \leq 0.05$, **$0.005 \leq p \leq 0.01$, ***$p < 0.005$, two-tailed
1012 Students t-test; comparison to mock).

1013

1014 **Fig. 2.**

1015 The expression levels of distinct pro-apoptotic genes increase following knockdown
1016 of TRF2. *Drosophila* S2R+ cells were incubated for three days with dsRNA directed
1017 against TRF2, exd, TBP and TRF1. RNA was isolated from the cells and reverse
1018 transcribed to cDNA. qPCR experiments were used to analyze the RNA levels of the
1019 endogenous genes: **a** *Trf2*, *TBP, TRF1*, *rpr*, *hid*, *grim*, *scyl*, *Buffy*, *Debcl* and *Dronc*
1020 and **b** *Trf2*, *p53* and *TBP.* qPCR experiments were performed in triplicates, and the
1021 graph represents the average of three to eight experiments. Error bars represent the
1022 SEM. *$p < 0.05$, one-way ANOVA followed by Tukey's post hoc test as compared to
1023 the mock treatment of the relevant gene.

1024

1025 **Fig. 3.**

1026 *Trf2*, but not *Tbp* or *Trf1* knockdown, affects cell cycle distribution. *Drosophila* S2R+
1027 cells were incubated for three days with dsRNA directed against *Trf2*, *Tbp*, *Trf1* and
1028 *exd*. Cells were fixed with 80% ethanol and stained with Propidium-Iodide (PI) for

1029 flow cytometry (FACS) analysis. **a** Cell cycle distribution histograms of a
1030 representative experiment. **b** Average cell cycle distribution determined by FACS
1031 analyses of eight independent experiments (*$0.01 < p \leq 0.05$, **$0.005 \leq p \leq 0.01$, ***p
1032 < 0.005, two-tailed Students t-test; comparison to mock).
1033
1034 **Fig. 4.**
1035 TRF2 is involved in S phase progression. *Drosophila* S2R+ cells were incubated for
1036 three days with dsRNA probes directed against *Trf2* or *Tbp*. Next, cells were either
1037 left untreated or treated with 1mM Hydroxyurea for 18h. The cells were allowed to
1038 resume cell cycle for 2h, 4h, 6h or 8h in fresh medium containing 40μM 5-Bromo-2´-
1039 deoxyuridine (BrdU), and were then fixed with 80% ethanol overnight and analyzed
1040 by FACS using BrdU-PI staining. Each histogram plots the PI fluorescence intensity
1041 (representing DNA content) on the X-axis, and cell count on the Y-axis.
1042
1043
1044 **Fig. 5.**
1045 Knock down of *Trf2* expression by RNAi reduces the expression of cyclin genes.
1046 *Drosophila* S2R+ cells were incubated for three days with dsRNA probes directed
1047 against *Trf2*, *exd*, *Tbp* and *Trf1*. RNA was isolated from the cells and reverse
1048 transcribed (RT) to cDNA. Real-time PCR (qPCR) experiments were used to analyze
1049 the RNA levels of the endogenous genes: **a** *Trf2*, *CycA*, *CycB*, *CycB3*, *CycC*, *CycD*
1050 and **b** *CycE*. As there were differences in *CycE* expression following RNAi with
1051 probe #1 compared to probe #2, four non-overlapping probes were used to
1052 knockdown *Trf2* expression towards the analysis of *CycE* expression. qPCR
1053 experiments were performed in triplicates, and the graph represents the average of

1054 three to eight experiments. Error bars represent the SEM. *p< 0.05, one-way
1055 ANOVA followed by Tukey's post hoc test as compared to the mock treatment of the
1056 relevant gene. **c** Western blot analysis following TRF2 and TBP knockdown in S2R+
1057 cells, using anti-TRF2 polyclonal antibodies and anti-Cyc E monoclonal antibodies.
1058 Actin was used as a loading control.
1059
1060 **Fig. 6.**
1061 TRF2 regulates cell cycle progression through mitosis. *Drosophila* S2R+ cells were
1062 incubated for three days with dsRNA directed against TRF2 or TBP. Cells were then
1063 fixed with 4% PFA and stained with a phospho-Histone H3 (Ser10) antibody (PH3,
1064 mitotic marker; green), Hoechst (DNA visualization; Blue) and Phalloidin (filamentous
1065 Actin visualization; red). **a** Representative confocal microscopy images of *Drosophila*
1066 S2R+ cells in different mitotic phases. **b** Comparison of mitotic indices following each
1067 treatment, calculated based on microscopic analysis. Shown are the averages of
1068 three independent experiments, in which a total of 100,000-800,000 cells were
1069 analyzed for each treatment (*$0.01 < p \leq 0.05$, **$0.005 \leq p \leq 0.01$, ***$p < 0.005$, two-
1070 tailed Students t-test; comparison to mock). **c** Representative images obtained by
1071 imaging flow cytometry analysis. **d** Comparison of mitotic indices following each
1072 treatment, calculated based on imaging flow cytometry. Shown are the averages of
1073 three independent experiments, in which a total of 40,000 cells were analyzed for
1074 each treatment (*$0.01 < p \leq 0.05$, **$0.005 \leq p \leq 0.01$, ***$p < 0.005$, two-tailed
1075 Students t-test; comparison to mock). **e-f** Distribution of mitotic phases among all
1076 mitotic cells, based on imaging flow cytometry. Shown are the averages of three
1077 independent experiments, in which a total of 40,000 cells were analyzed for each
1078 treatment (*$0.01 < p \leq 0.05$, **$0.005 \leq p \leq 0.01$, ***$p < 0.005$, two-tailed Students t-

1079 test; comparison to mock). Filled triangles indicate aberrant chromosomal
1080 morphology in Colchicine-treated cells. Phospho-Histone H3 Ser10-positive cells (**e**),
1081 were analyzed separately from the Phospho-Histone H3 Ser10-negative cells
1082 undergoing mitosis (**f**). Phospho-Histone H3 Ser10-negative cells undergoing mitosis
1083 (as identified by the imaging flow cytometer) were defined as cells in telophase (f).
1084 Notably, cell counts of telophase cells likely include Phospho-Histone H3 Ser10-
1085 negative doublet cells, which, even using the high-resolution Imagestream, could not
1086 be distinguished from telophase cells.
1087
1088 **Fig. 7.**
1089 *CycA* and *CycB* expression is affected by TRF2 knockdown, and less by GFZF and
1090 M1BP. **a** Schematic representation of genes containing at least one binding site of
1091 the specified transcription factor at ±50bp relative to its TSS, as determined by
1092 FlyBase. ChIP-exo data was retrieved from GSE97841 and GSE105009. **b** Top
1093 enriched motif among the 4331 commonly bound promoters, as detected by MEME
1094 analysis. Its resemblance to Ohler Motif 1 is depicted by the motif logo derived by
1095 M1BP ChIP-exo (57). **c** The 4331 commonly bound regions were analyzed for core
1096 promoter composition. This promoter group was found to be depleted for the TATA-
1097 box motif and enriched for dTCT and the Motif 1 core promoter elements. p-values
1098 were adjusted using Bonferroni correction. ***$p < 10^{-5}$. **d-e** *Drosophila* S2R+ cells
1099 were incubated for three days with dsRNA probes directed against *Trf2* (probe #1),
1100 *gfzf*, *M1BP* or their combinations. RNA was isolated from the cells and reverse
1101 transcribed (RT) to cDNA. Real-time PCR (qPCR) experiments were used to analyze
1102 the RNA levels of the endogenous of *Trf2*, *gfzf* and *M1BP*, as well as *CycA*, *CycB*,
1103 *CycD* and *CycE* genes, as indicated. **d** Single knockdowns of *Trf2*, *gfzf* or *M1BP.* **e**
1104 Knockdown of multiple genes, as indicated. qPCR experiments were performed in

1105 triplicates, and the graph represents the average of 4 independent experiments.
1106 Error bars represent the SEM. *p< 0.05, one-way ANOVA followed by Tukey's post
1107 hoc test as compared to the mock treatment of the relevant gene.
1108
1109

1110 **Additional files**

1111 **Additional file 1: Figure S1. .pdf**

1112 *A*) Schematic representation of dsRNA TRF2 probes used in this study. *B*) Western
1113 blot analysis following TRF2 and *C)* TBP knockdown in S2R+ cells, using anti-TRF2
1114 and anti-TBP polyclonal antibodies, respectively. Actin and γ-Tubulin were used as
1115 loading controls.

1116 **Additional file 2: Table S1. .xlsx**
1117 GO terms analysis of the RNA-seq data. Summary, as well as the exact GO terms
1118 are provided, according to the datasheet name. Analysis was performed sing
1119 STRING. Only genes with pAdj <0.1 were considered. DEseq2 output is presented
1120 for either *Trf2* or *Tbp* knockdown, as compared to mock at 72h post silencing.
1121

1122 **Additional file 3: Figure S2. .pdf**
1123 TBP overexpression does not result in induction of pro-apoptotic gene expression.
1124 *Drosophila* S2R+ cells were depleted of *Trf2* by RNAi and then transfected with
1125 either pAc-empty (mock) or TBP expression vector. Cells were harvested 36–48h
1126 following transfection, RNA was purified and reverse transcribed to cDNA for RT-
1127 qPCR analysis. qPCR experiments were performed in triplicates, and the graph
1128 represents the average of 3 experiments. Error bars represent the SEM. *p< 0.05,

1129 two-tailed Students t-test; comparison to the same treatment without TBP
1130 overexpression.
1131

1132 **Additional file 4: Figure S3. .pdf**

1133 TRF2 is involved in S phase progression. *Drosophila* S2R+ cells were incubated for
1134 three days with dsRNA probes directed against *Trf2* or *Tbp*. Next, cells were either
1135 left untreated or treated with 1mM Hydroxyurea for 18h. The cells were allowed to
1136 resume cell cycle for 2h, 4h, 6h or 8h in fresh medium containing 40μM BrdU, and
1137 were then fixed with 80% ethanol overnight and analyzed by FACS using BrdU-PI
1138 staining. The PI fluorescence intensity (representing DNA content) is plotted on the
1139 X-axis (linear scale), and the BrdU-FITC fluorescence intensity (representing BrdU
1140 incorporation into the DNA) is plotted on the Y-axis (log scale).
1141

1142 **Additional file 5: Figure S4. .pdf**

1143 Gating and masking strategy for imaging-flow cytometry data analysis. *A*) Cells were
1144 gated for single cells, using the area and aspect ratio features on the BF image. *B*)
1145 Centered and uncropped cells were gated based on the centroid X (the number of
1146 pixels in the horizontal axis from the upper left corner of the image to the center of
1147 the mask) and area features. *C*) Focused cells were gated, using the Gradient RMS
1148 feature, as previously described (78). *D*) The G2/M population was gated out of the
1149 focused cells, based on DNA (Hoechst) intensity. *E*) Mitotic cells were gated from the
1150 G2M population, as the high intensity population of pH3 staining, based on the
1151 intensity feature of pH3 and Max pixel feature of pH3 (the largest value of the
1152 background-subtracted pixels contained in the input mask). *F*) To include only single
1153 positive pH3 stained cells, doublet cells were eliminated by gating the single cells

1154 from the mitotic population, using the area and aspect ratio features of the BF. *G*) To
1155 discriminate between the different mitotic phases subpopulations, several masks
1156 were created: 1. A morphology mask that includes all pixels within the outermost
1157 image contour. 2. A threshold mask that includes the highest intensity pixels
1158 (indicated as percentages). 3. A range mask that selects components in an image
1159 within a selected size (μm), was used to eliminate small components.
1160 Furthermore, the following features were used on the combined masks:
1161 1. Spot count - the number of connected components in an image.
1162 2. Aspect ratio intensity - the aspect ratio weighted for fluorescence intensity.
1163 These masks were combined and the features were calculated and plotted as
1164 follows:
1165 Spot count of the combined mask: range (threshold 75%, M07) 20-5000, was plotted
1166 against the aspect ratio intensity of the combined mask: range
1167 (Threshold(Morphology(M07), 82%) 15-5000.
1168 The prophase population was defined as having a more circular nuclear staining
1169 (aspect ratio intensity should be high), and was hence gated as one nuclear spot
1170 count with aspect ratio intensity bigger than 0.6. On the other hand, the metaphase
1171 population was defined as having a more elongated DNA distribution and was gated
1172 as one nuclear spot count with aspect ratio intensity smaller than 0.6. Finally, the
1173 anaphase population was gated as cells with two nuclear spots having aspect ratio
1174 intensity less than 0.6. (80). *H*) As serine 10 of histone H3 becomes
1175 dephosphorylated during telophase, the telophase population was derived from the
1176 negative pH3-stained cells. To identify telophase pairs, an object mask was created
1177 (which segments images to closely identify the area corresponding to the cell). The
1178 circularity feature (which measures the degree of the mask's deviation from a circle)

1179 of the object mask (BF), was plotted against the aspect ratio intensity of the M07
1180 DNA mask. Telophase cells were gated as having the lowest BF circularity and as
1181 the most elongated, based on DNA stain (lowest aspect ratio intensity (M07)).
1182
1183 **Additional file 6: Table S2. .doc**
1184 Number of cells in each mitotic phase within phospho-Histone H3 Ser10-positive
1185 mitotic cells or telophase.
1186
1187 **Additional file 7: Figure S5. .pdf**
1188 *Drosophila* S2R+ cells treated with Colchicine display aberrant chromosomal
1189 morphology. Colchicine-treated cells were fixed with 4% PFA and stained with a
1190 phospho-Histone H3 (Ser10) antibody (green), Hoechst (DNA visualization; blue)
1191 and Acti-stain 670 Phalloidin (filamentous Actin visualization; red). *A*) Shown are
1192 representative images of cells in different mitotic phases obtained by imaging flow
1193 cytometry analysis. *B*) Quantitation of cells with aberrant DNA morphology within
1194 mock and colchicine-treated cells using imaging flow cytometry analysis. Prophase-
1195 and metaphase-gated cells within either mock or colchicine-treated S2R+ cells, were
1196 further gated using calculations of the following features:
1197 1. The Delta centroid XY feature (which measures the distance in microns between
1198 the centroid feature of two images using the user provided masks) was calculated
1199 using the BF default mask and Hoechst channel mask of the 60% most highly
1200 intense pixels. Cells with centered nucleus will get a lower value while polar located
1201 nucleus will get a higher value. 2. The Max contour position feature (the location of
1202 the contour in the cell that has the highest intensity concentration; the score is
1203 between 0 to 1, with 0 being the object center and 1 the object perimeter). To

1204 distinguish between central vs. polar location of the dividing nucleus, the Delta-
1205 centroid XY was plotted against the Max contour position, and polar DNA was gated
1206 as having the highest values of both features. Depicted are the analyses of cells in
1207 prophase and metaphase. Cells in anaphase are not shown due to the low number
1208 of cells observed in anaphase (Additional file 6).
1209
1210 **Additional file 8: Table S3. .xlsx**
1211 Mass-spectrometry data for short TRF2, long TRF2 and TBP proteins.
1212
1213 **Additional file 9: Figure S6. .pdf**
1214 Knockdown of *M1BP* specifically elevates the expression of *CycA* and ribosomal
1215 protein genes. *Drosophila* S2R+ cells were incubated for three days with dsRNA
1216 probes as indicated in the legend. RNA was isolated from the cells and reverse
1217 transcribed (RT) to cDNA. Real-time PCR (qPCR) experiments were used to analyze
1218 the RNA levels of the endogenous genes. qPCR experiments were performed in
1219 triplicates, and the graph represents the average of 3 experiments ± SEM. *A) CycA*
1220 expression levels are reduced following *Trf2* knockdown, but not *gfzf* or *M1BP*
1221 knockdown. *$p < 0.05$, one-way ANOVA followed by Tukey's post hoc test as
1222 compared to the mock treatment of the relevant gene. *B)* Additional ribosomal genes
1223 are influenced by *M1BP* knockdown, however not all genes are upregulated in
1224 response to *M1BP* knockdown. *CG12493* and *sgll* genes were previously shown to
1225 be downregulated upon *M1BP* knockdown (62).**$p < 0.01$, two-tailed Students t-test;
1226 compared to mock treatment.
1227

Table 1.

Primers for generation of dsRNA probes

dsRNA probe	Forward primer	Reverse primer
Trf2 #1	ATAGGTACCGGCAACCGGCAGTAAAAATA	ATAACTAGTACTCCACATTTGATCCCTGC
Trf2 #2	ATACTCGAGAACAGAAGGAGCAGCATCGT	ATAACTAGTTATTTTTACTGCCGGTTGCC
Trf2 #3	ATAGGTACCAAGGAGAACCAATCGCCGAAT	ATAACTAGTATTAGAAGAACTTAAGCGATC
Trf2 #4	ATACTCGAGCAATCTGACTTGAATCCCGG	ATAACTAGTTCATCTGAAGCTTGTCGCG
exd	ATAACTAGTTCGATGGTGCTGACAATGCC	ATAGGTACCGGGGCTTAGATCCTGATGGAG
Trf1	GGGGTACCGGACAGGGATAATGTGGCTG	AAACTAGTGGCTTGACCATGCGATAGAT
Tbp	GGGGTACCACATGATGCCCATGAGTGA	AAACTAGTAATGGGGAATATCTTGTCGAAG
rpr	AAGGTACCACGAAAGAAAAGTGTGTGCG	AAACTAGTTGCAATTTTTAGCCAACTTCG
scyl	AAGGTACCTACTACGCTGCTGACGAGGA	AAACTAGTATCACCATTAGTTGGTGGGCG
p53	AAGGTACCGATGCTGCAGGACATTCAGA	AAACTAGTCTCGGCTATCATTGCTCTCC
M1BP	GGGGTACCATATTAACACGAAACACCGGG	AAACTAGTACCTTGGTGTCGTCGATCTC
gfzf	GGGGTACCTCAGCATCTGTTCCACTTCG	AAACTAGTGTGTGTGAATGTGGGTCGAG

Table 2.

Real-time PCR (qPCR) primers

Gene	Forward primer	Reverse primer
Gapdh2	TTCCTCAGCGACACCCACTC	ATGACGCGGTTGGAGTAGCC
Trf2	GGAATCGTCTTCTGGGGACT	GACGACTCCTGTTGGCTTTG
CycA	TGGGCACGGCAGCTATGTAT	CCTGCGCCTTGGTGTAACTG
CycB	CGAGCACCATACGATGTCCA	TTGAGCAAGTGCAGCGACAG
CycB3	TCCCAGAGACTGCTCCAAGC	CATGGCGTAGTGGGACACCT
CycC	CACCGATGTCTGCCTGCTC	GCACGATCTCCTGGACCTTG
CycD	AGGTCGAGGAGAAGCACCAC	CCTCGGCACACACTTCCAT
CycE	CTCGGTTTTGAGCCTCCATC	AGACAACGGGCGAGGTGTAG
Tbp	TCAGCTCCGGCAAGATGGTG	GCAGGGAAACCGAGCTTTTGG
Trf1	AGAAGCTGGGATTCCCCGTA	GCACGTGGTTGAGGTTCTCC
exd	GCGAAATCAAGGAGAAGACCGTCC	CCTCGGCAATCAGCATGTTGTCC
rpr	CATACCCGATCAGGCGACTC	GTGTACTGGCGCAGGGTTTC
hid	CGACCTCCACGCCGTTATC	GCTCTGGTACTCGCGCTCAT
grim	TTTGGCCCAGATCTTCTGCT	GCATCAGTCACGTCGTCCTC
Debcl	ACAGCATGGGCGAGGAACT	ATGTCGCTGTCCTCCAGCTC
scyl	ATAATCCGCGTGTCGGAGAA	CCGTATCCGAATCGACCTTG
buffy	TTCTCAGGGTCGTTGCCTGT	TGGAGGTGGAGCCCAGTATG
p53	TTAGCGTTGAGCCTTTGACG	CAGGGGGACTACAACGGAAA
M1BP	AATTTGGCTGCGAACTCTGT	CAGCGGCCACAGTACTTACA
gfzf	GAACCCACCGGATATGTCAC	TGCTGGCAGGGTCTTAAGTT
RpLP2	GACATGGGCTTCGCTCTCTT	GTGAACGGATGGGTGCTACA
RpS12	CAAGCGTCAGGCTGTTCTGT	CAGCTTCTTGTGCGAGTCCA
CG12493	GACAACCAATTGGATCAGGAAAG	AGATTCACCATCGGGCATATT
sgll	ATTCGAAGGATGAGCCAAGG	CCAGTCTCGGAATACACAGAAG
RpL30	CAAATACTGCCTGGGCTACA	TACTCGATCTCGGACTTCCTC
RpLP1	CACTTCGACATGTCCACCAA	CCTTCAGGATGGTGTTGATCTT

Table 3.

Enrichment of TRF2, TBP, M1BP and GFZF in FLAG-immuno-affinity purified complexes from inducible S2R+ cells

Name of purified (/co-purified) protein	Enrichment of purified (/co-purified) proteins within		
	Short TRF2-associated proteins	Long TRF2-associated proteins	TBP-associated proteins
TRF2	78.695	6.128	-
TBP	-	-	18.3
M1BP	1.795E7	-	-
GFZF	1.683E7	-	-

The values in the table represent the enrichment of each purified (/co-purified) protein in the indicated sample. The enrichment was calculated as the ratio between the mass spectrometry area (the average of the three most intense peptides from each protein) of the induced sample and the un-induced sample.

Table 4.

TRF2, M1BP and GFZF occupancy within -100 to +100 relative to the TSSs

Gene name	TSS Location	TRF2			M1BP			GFZF		
		# of bound sites	Max. peak score	Avg. peak score	# of bound sites	Max. peak score	Avg. peak score	# of bound sites	Max. peak score	Avg. peak score
CycA_1	chr3L:11826617	1	54.16	54.16	59	126.93	30	2	112.85	87.78
CycA_2	chr3L:11826310	1	36.11	36.11	1	20.04	20.04	0	0	0
CycB_1	chr2R:18694432	15	150.45	38.11	47	106.89	26.72	3	114.64	62.1
CycB_2	chr2R:18694437	15	150.45	38.11	51	106.89	25.28	3	114.64	62.1
CycB_3	chr2R:18694449	15	150.45	38.11	60	106.89	27.28	3	114.64	62.1
CycB3	chr3R:20696533	4	90.27	40.62	128	140.29	36.69	9	157.63	72.05
CycE_1	chr2L:15746609	2	66.2	42.13	1	6.68	6.68	0	0	0
CycE_2	chr2L:15748123	4	60.18	31.6	8	53.44	30.9	1	136.14	136.14
CycC_1	chr3R:10715915	4	36.11	24.07	4	66.81	23.38	1	42.99	42.99
CycC_2	chr3R:10715922	4	36.11	24.07	3	66.81	26.72	1	42.99	42.99
CycD_1	chrX:15803691	2	42.13	24.08	7	46.76	20.04	0	0	0
CycD_2	chrX:15803682	2	42.13	24.08	7	46.76	20.04	0	0	0
RpL5	chr2L:22429377	74	210.63	51.56	142	140.29	33.07	29	148.68	48.36
RpL7	chr2L:10201108	23	210.63	50.50	121	374.11	62.44	5	118.23	65.92
RpL23	chr2R:18741912	38	132.4	46.25	200	327.35	51.27	68	449.61	99.00
RpL30	chr2L:19009229	21	102.31	30.38	141	233.82	47.81	16	231.08	76.58
RpLP1	chr2L:419957	14	156.47	44.28	148	180.38	37.78	19	195.25	74.10
RpLP2	chr2R:12473638	48	234.71	67.08	175	173.70	37.37	8	175.55	65.16

TRF2, M1BP and GFZF occupancy data (number of bound sites, the maximum peak scores and the average peak scores) was retrieved from ChIP-exo experiments performed in *Drosophila* S2R+ cells (GSE97841 and GSE105009) (64, 65). Due to variations in TSSs obtained by different methods, we relate to -100 to +100 relative to the TSSs peaks from available 5'GRO-seq and focused TSS analysis in S2 cells (GSE68677 and http://labs.biology.ucsd.edu/Kadonaga/drosophila.tss.data/) and PRO-cap analysis in S2 cells (GSM1032759).

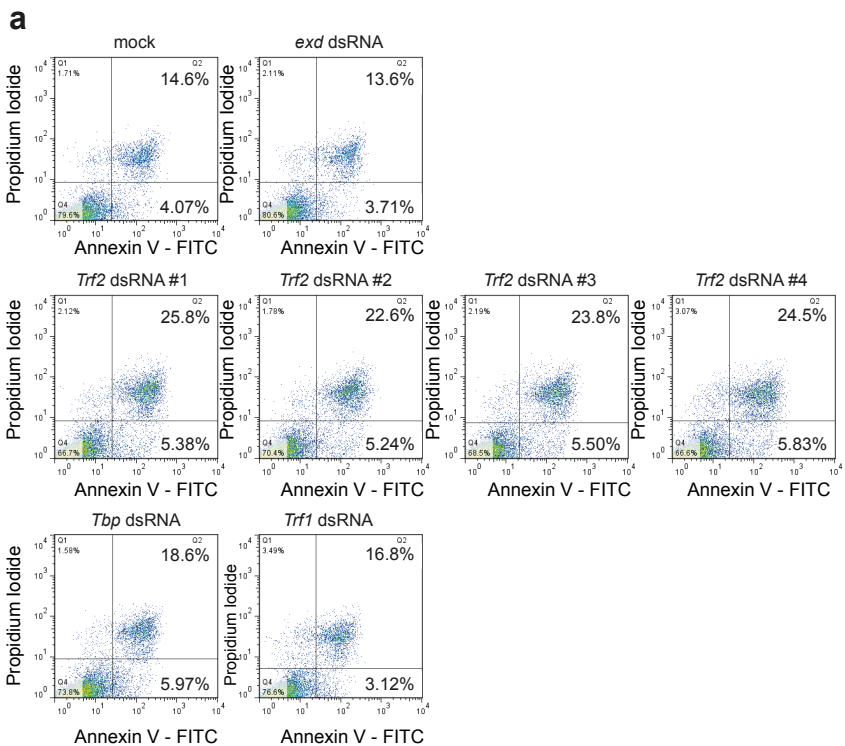
a
mock
14.6%
4.07%
exd dsRNA
13.6%
3.71%
Trf2 dsRNA #1
25.8%
5.38%
Trf2 dsRNA #2
22.6%
5.24%
Trf2 dsRNA #3
23.8%
5.50%
Trf2 dsRNA #4
24.5%
5.83%
Tbp dsRNA
18.6%
5.97%
Trf1 dsRNA
16.8%
3.12%
Propidium Iodide
Annexin V - FITC

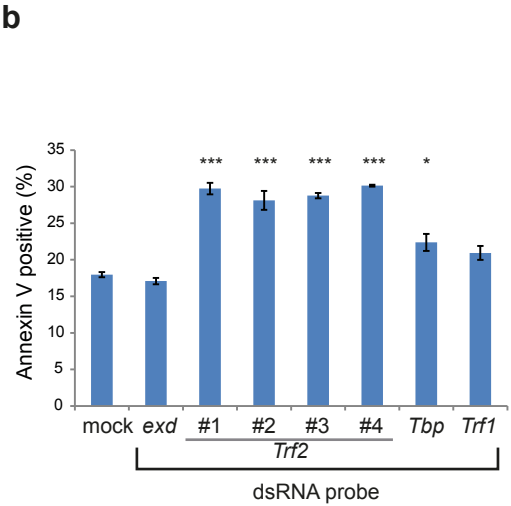
b
Annexin V positive (%)
35
30
25
20
15
10
5
0
***
***
***
***
*
mock
exd
#1
#2
#3
#4
Tbp
Trf1
Trf2
dsRNA probe

Kedmi et al._Fig. 2

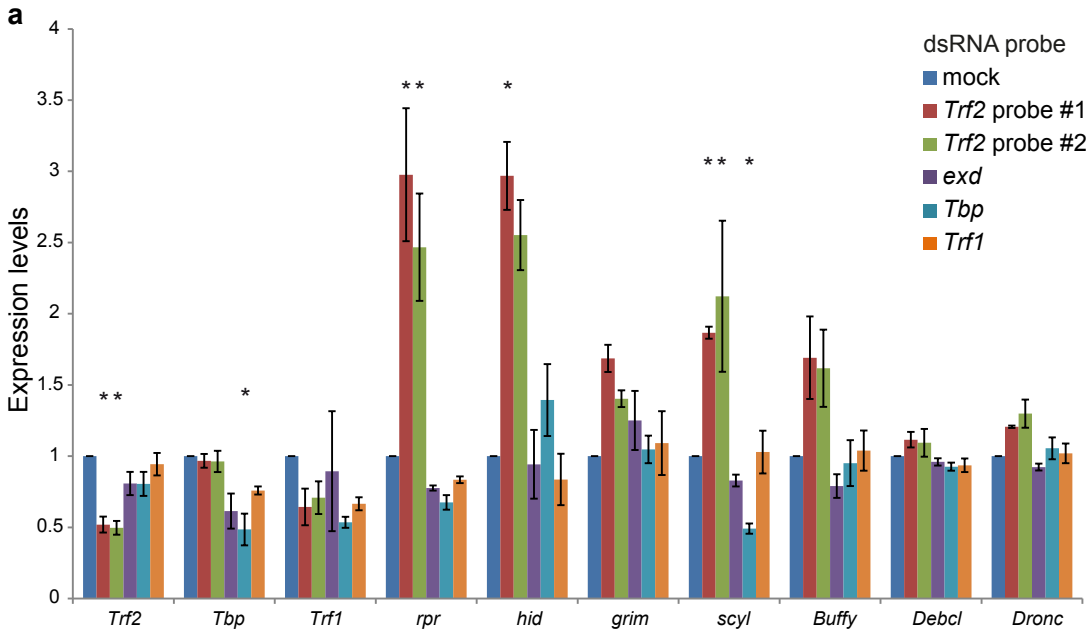

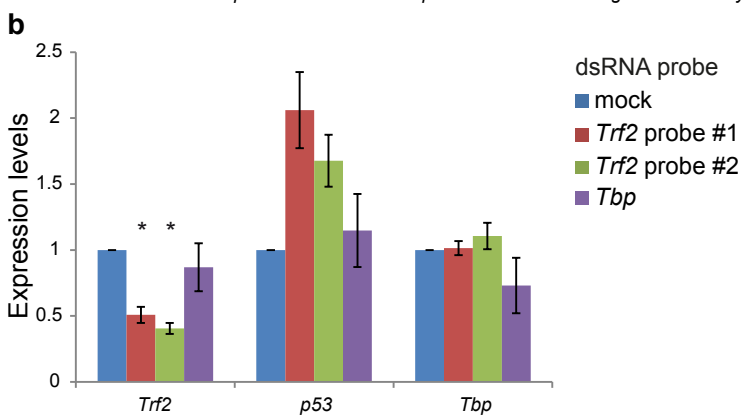

Kedmi et al._Fig. 3

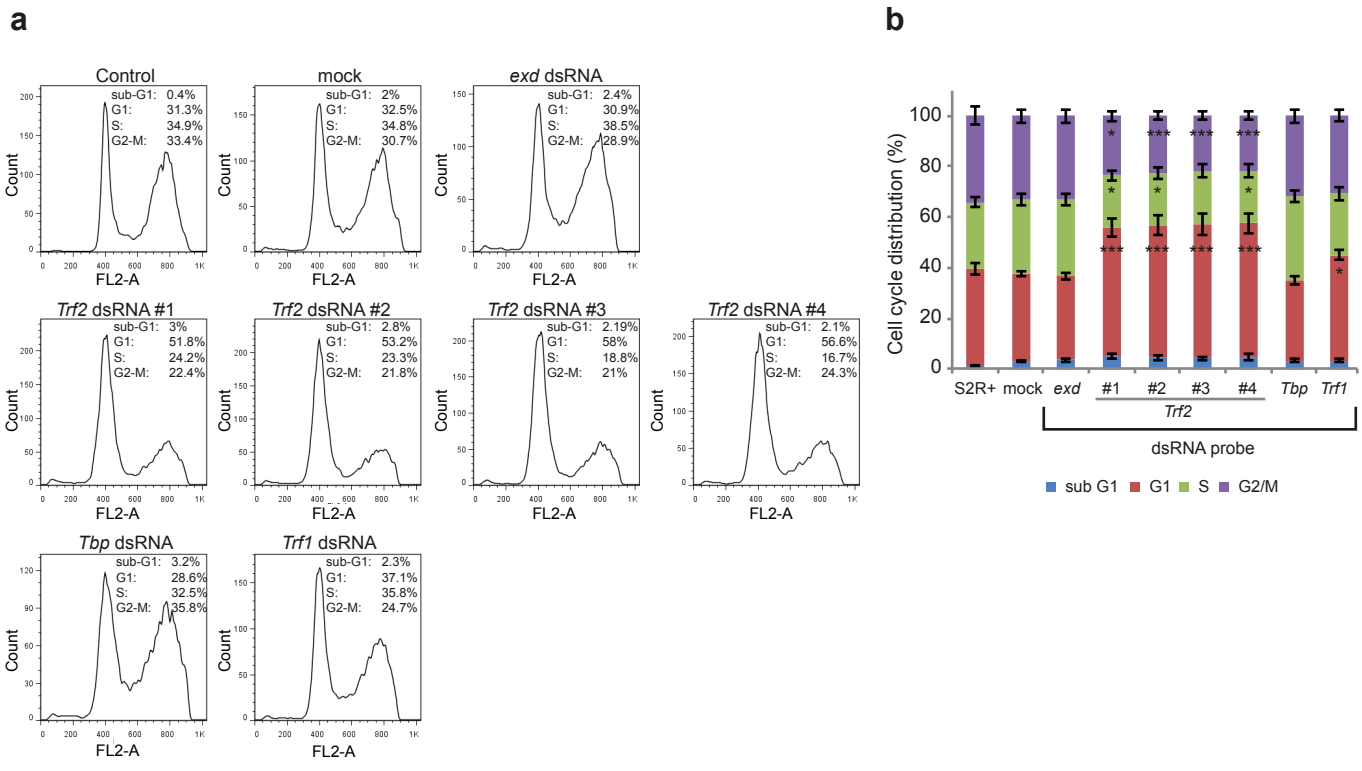

Kedmi et al._Fig. 4

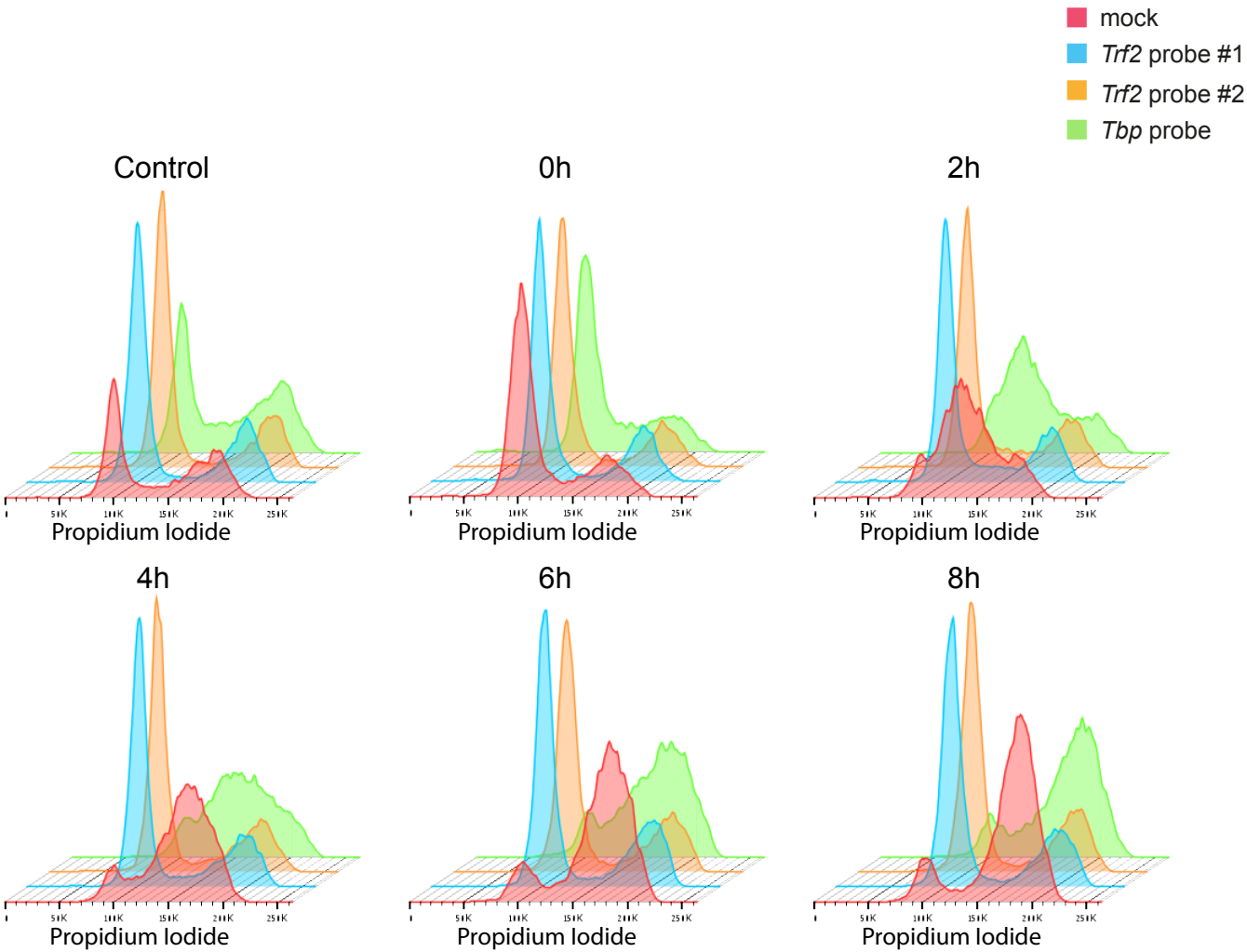

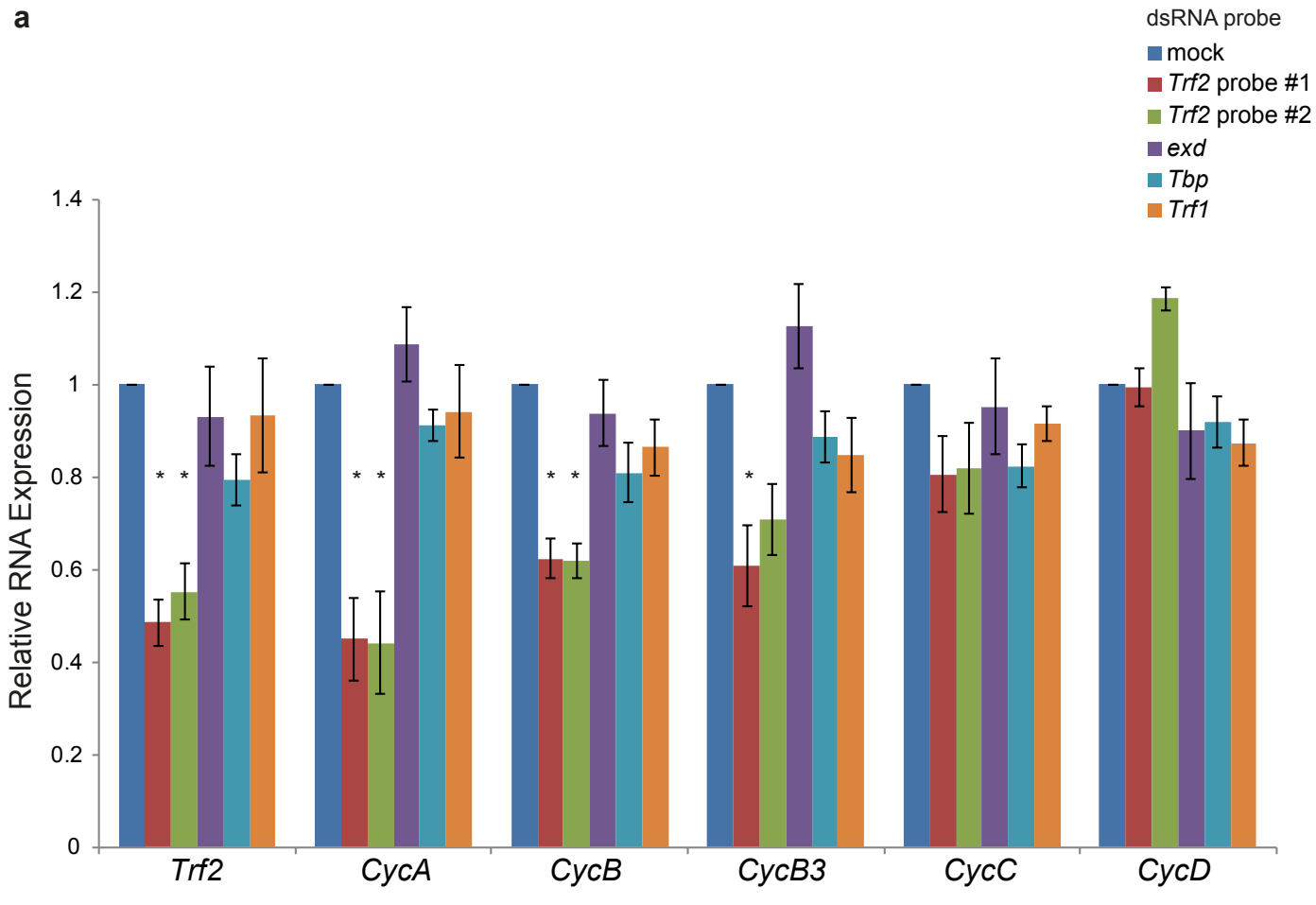
a
dsRNA probe
mock
Trf2 probe #1
Trf2 probe #2
exd
Tbp
Trf1
Relative RNA Expression
1.4
1.2
1
0.8
0.6
0.4
0.2
0
Trf2
CycA
CycB
CycB3
CycC
CycD

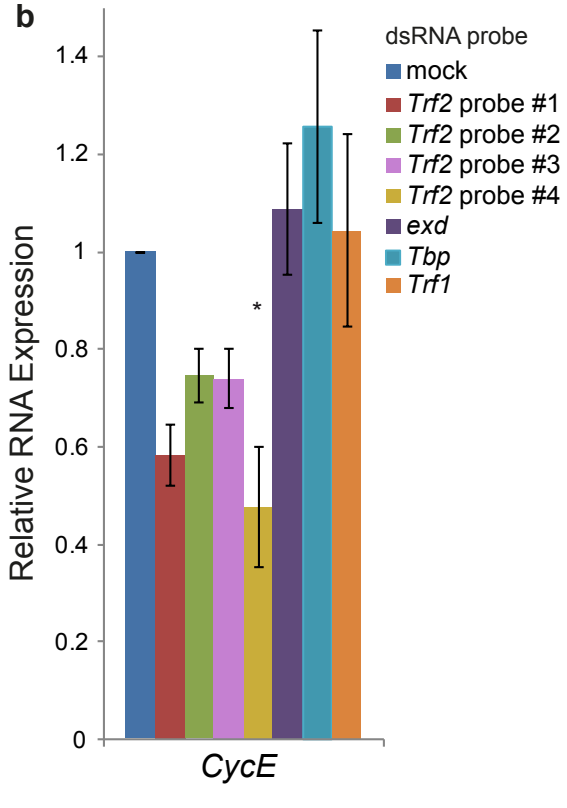
b
dsRNA probe
mock
Trf2 probe #1
Trf2 probe #2
Trf2 probe #3
Trf2 probe #4
exd
Tbp
Trf1
Relative RNA Expression
1.4
1.2
1
0.8
0.6
0.4
0.2
0
CycE

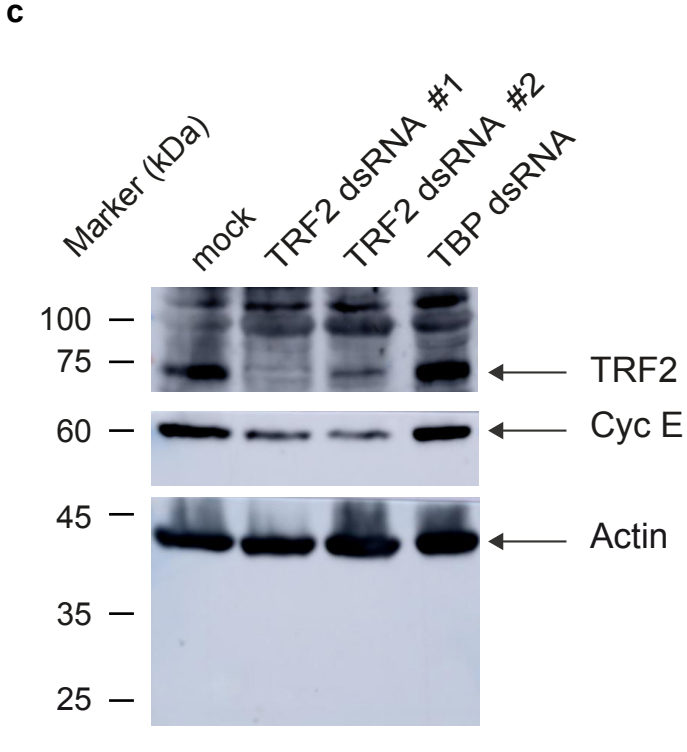
c
Marker (kDa)
mock
TRF2 dsRNA #1
TRF2 dsRNA #2
TBP dsRNA
100
75
60
45
35
25
TRF2
Cyc E
Actin

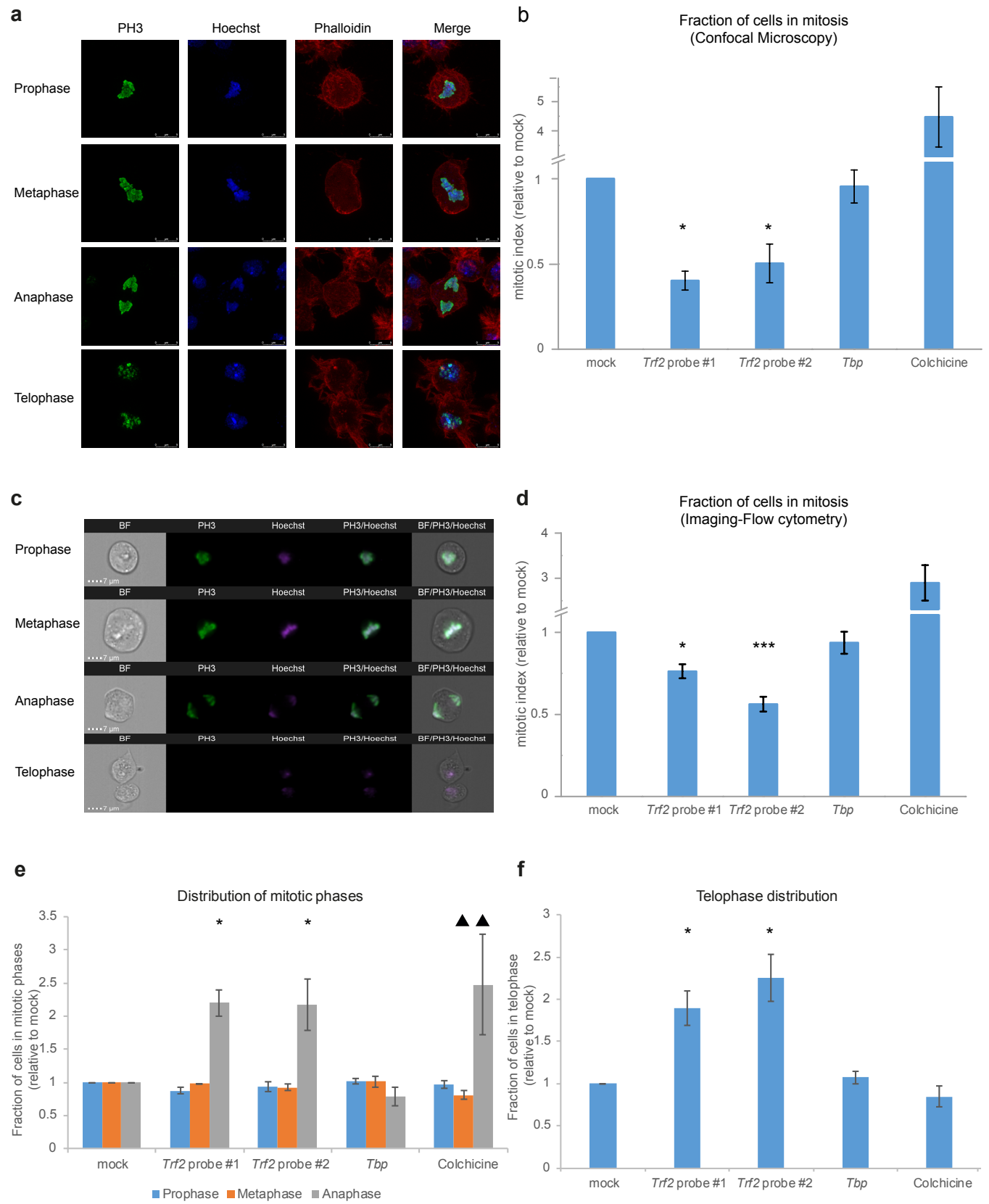
a
PH3
Hoechst
Phalloidin
Merge
Prophase
Metaphase
Anaphase
Telophase
b
Fraction of cells in mitosis
(Confocal Microscopy)
mitotic index (relative to mock)
mock
Trf2 probe #1
Trf2 probe #2
Tbp
Colchicine
c
BF
PH3
Hoechst
PH3/Hoechst
BF/PH3/Hoechst
Prophase
Metaphase
Anaphase
Telophase
d
Fraction of cells in mitosis
(Imaging-Flow cytometry)
mitotic index (relative to mock)
mock
Trf2 probe #1
Trf2 probe #2
Tbp
Colchicine
e
Distribution of mitotic phases
Fraction of cells in mitotic phases
(relative to mock)
mock
Trf2 probe #1
Trf2 probe #2
Tbp
Colchicine
Prophase
Metaphase
Anaphase
f
Telophase distribution
Fraction of cells in telophase
(relative to mock)
mock
Trf2 probe #1
Trf2 probe #2
Tbp
Colchicine

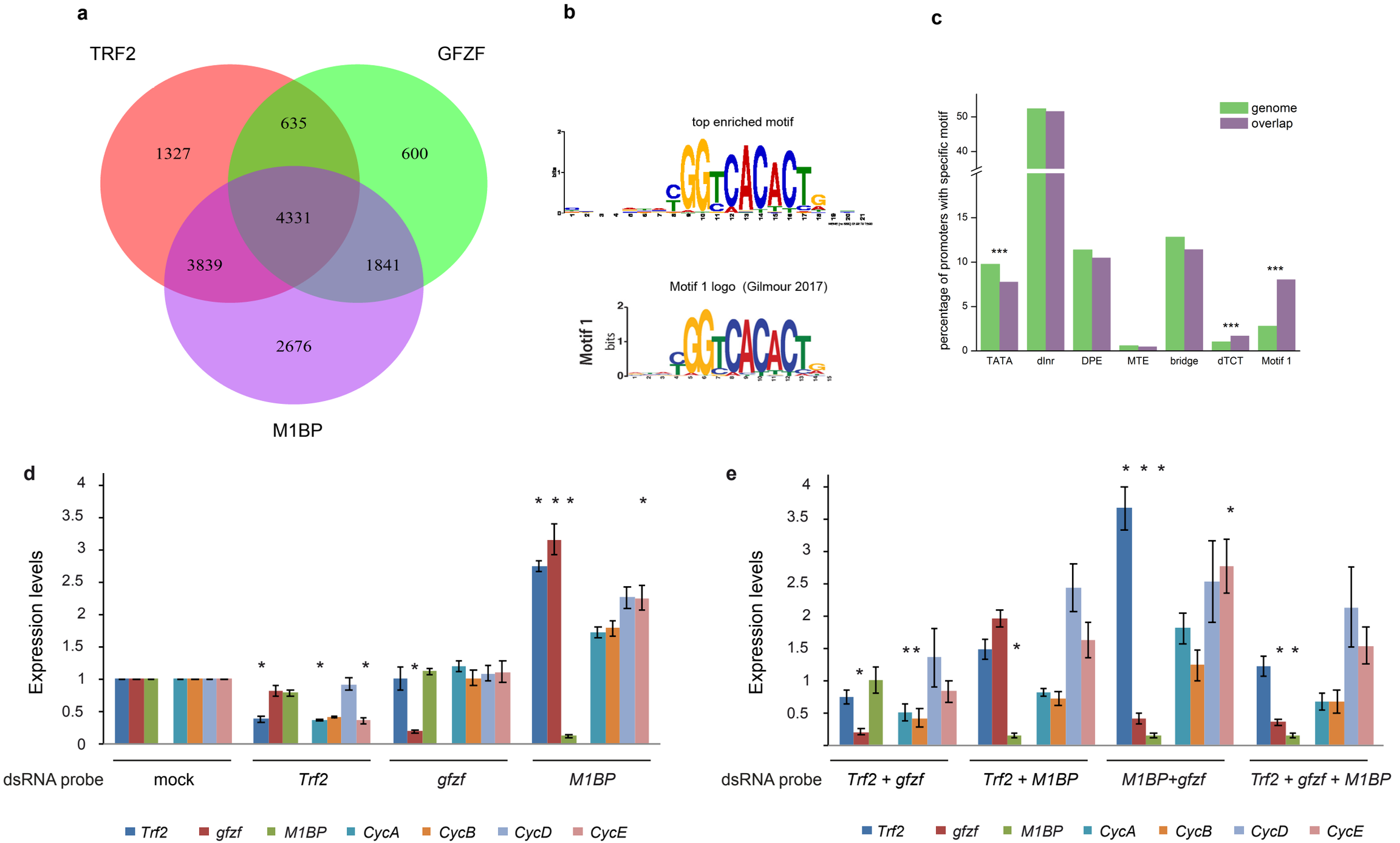
a
TRF2
GFZF
M1BP
1327
635
600
4331
3839
1841
2676
b
top enriched motif
Motif 1 logo (Gilmour 2017)
Motif 1
bits
c
genome
overlap
percentage of promoters with specific motif
TATA
dInr
DPE
MTE
bridge
dTCT
Motif 1
d
Expression levels
dsRNA probe
mock
Trf2
gfzf
M1BP
Trf2
gfzf
M1BP
CycA
CycB
CycD
CycE
e
Expression levels
dsRNA probe
Trf2 + gfzf
Trf2 + M1BP
M1BP+gfzf
Trf2 + gfzf + M1BP
Trf2
gfzf
M1BP
CycA
CycB
CycD
CycE